https://doi.org/10.1016/j.trb.2020.06.004

Green technology adoption for fleet deployment in a shipping network

Lu Zhen[a], Yiwei Wu[a], Shuaian Wang[b,*], Gilbert Laporte[c]

[a] *School of Management, Shanghai University, Shanghai, China*
[b] *Department of Logistics & Maritime Studies, The Hong Kong Polytechnic University, Kowloon, Hong Kong*
[c] *Department of Decision Sciences, HEC Montréal, Montréal, Canada*

Abstract

The Emission Control Areas (ECAs) established by the International Maritime Organization are beneficial to reduce the sulphur emissions in maritime transportation but bring a significant increase in operating cost for shipping liners. Low sulphur emissions are required when ships berth or sail within ECAs. It is an irreversible trend that green technologies such as scrubbers and shore power will be implemented in maritime shipping industry. However, the literature lacks a quantitative decision methodology on green technology adoption for fleet deployment in a shipping network in the context of ECAs. Given a shipping network with multiple routes connected by transshipment hubs, this study proposes a nonlinear mixed integer programming model to optimally determine fleet deployment along routes (including green technology adoption), sailing speeds on all legs, timetables, cargo allocation among routes for each origin-destination pair, and berth allocation considering the availability of shore power at different berths in order to minimize total five types of cost. A three-phase heuristic is also developed to solve this problem. Numerical experiments with real-world data are conducted to validate the effectiveness of the proposed model and the efficiency of the three-phase heuristic. Some managerial implications are also outlined on the basis of the numerical experiments.

Keywords: Liner shipping management; fleet deployment; emission control area; green technology adoption; scrubbers; shore power.

*Corresponding author. wangshuaian@gmail.com (S. Wang)

Preprint submitted to Transportation Research Part B: Methodological *April 7, 2020*

1. Introduction

Although shipping is considered to be an environmentally efficient mode of transportation, it also releases tremendous pollution emissions that have harmful influences on human health and on the global environment. Shipping is estimated to account for 5–7% of the global SO_X emissions (Ren and Lützen, 2015). In order to reduce global sulphur emissions from ships when they are operating near coasts, the International Maritime Organization (IMO) promulgated Emission Control Area (ECA) regulations that are described in the MARPOL Annex VI in 2015 (IMO, 2016). The latest ECA regulations require that ships sailing inside the ECAs in the Baltic Sea, the North Sea, North America, and the Caribbean Sea, use marine bunkers with a sulphur content of no more than 0.1% or take equivalent measures. Starting from 2019, China has established coastal emission control areas in which a 0.5% sulfur limit has been enforced. Moreover, the Marine Environment Protection Committee of the IMO decided to reduce the sulphur content worldwide to 0.5% from 2020 (IMO, 2016).

With strict emission regulations and more public focus on shipping transport, it is crucial for shipping companies to reduce emissions in a cost-effective way. Kontovas and Psaraftis (2011) and Wen et al. (2017) point out that speed reduction could be a tool for reducing emissions. Moreover, some companies' ships use low sulphur fuel oil, such as marine gas oil (MGO), when they sail and berth in the coastal ECA, which leads to an increase in operating costs. Scrubbers which absorb the sulphur oxides in a counterflow of seawater are also considered as an efficient method for sulphur removal because the installation of scrubbers on ships allows ships to keep using cheap high sulphur fuel oil, such as heavy fuel oil (HFO) within ECAs. Apart from the emissions caused by combustion of fossil fuels for propulsion, the power generation of a ship mooring at a berth also releases sulphur emissions (Sciberras et al., 2015). With stricter emission regulations and increasing environmental consciousness of shipping companies and port operators, shore power is becoming a more popular and feasible option. It refers to a technique called the high-voltage shore connection system used for locally emission-free solutions by having berthed ships plug into the shore electrical system (Khersonsky et al., 2007). If a ship equipped with shore power moors at a berth that is capable of providing shore power, this ship will use the shore power during the dwell duration for a locally emission-free solution. Otherwise, the ship will use the HFO or MGO according to the availability of scrubbers.

Compared with green technologies, the investment cost of fuel switch is relatively low but the operating cost is extremely high. In 2018, the average bunker price of MGO was 686.5 USD/ton, 57% higher than that of HFO, whose price was 437.0 USD/ton (Ship and Bunker, 2019). The China COSCO Shipping Group spent an extra amount of 27 million USD to burn MGO within ECAs in 2015 (Zhen et al., 2019c). If shipping companies do not adopt any green technologies, the operating costs of ships may increase dramatically. Hence, shipping companies may be willing to invest in green technologies, which are usually expensive. For instance, Jiang et al. (2014) point out that the capital costs of the scrubber installation are 9.2 million USD; and the investment costs for shore power on the sea ship side are generally 1.0 million USD, which is also expensive (Winkel et al., 2016). Therefore, the green technology adoption (i.e., scrubbers, and shore power) is a strategic decision, which acquires careful consideration and decision supports from some scientific methodologies.

This study is motivated by a real-world problem encountered in sustainable development. Since the above-mentioned emission reduction methods have different advantages and drawbacks, and the investments in certain technologies are enormous, the choice of a sulphur emission control method for a shipping company is complex and critical. Besides, the green technology selection for fleet deployment belongs to the long-term strategic level of shipping companies. Hence, shipping companies need scientific methods to determine the most suitable green technologies for fleet deployment in order to balance the trade-off between their fixed costs (such as investment costs and weekly operating costs) and variable costs (such as fuel costs).

Operational research-based planning techniques have, particularly in recent years, contributed to the green transportation through the use of various optimization models (Bektaş et al., 2019). However, few studies provide a quantitative decision methodology for this important problem. This paper investigates the influences of the fuel costs, green technologies' investment cost and ECA policy on the decisions of fleet deployment and green technology adoption, and proposes a quantitative method to solve this complicated problem. More specifically, this study proposes a nonlinear mixed integer programming (MIP) model to optimally determine fleet deployment along routes (including green technology adoption), sailing speeds on all legs, timetables, cargo allocation among routes for each origin-destination pair, and berth allocation considering the availability of shore power at different berths, with an objective incorporating initial investment and operating cost of ships, fuel cost, transshipment cost for transhipped containers, service level related penalty, as well as extra cost for berths without shore power. The reason for considering berth allocation decision lies in the heterogeneous berths with or without shore power generating equipment, which further affects the mooring cost of ships with or without shore power receiving equipment. Moreover, the widely used ship fuel cost cubic function (Brouer et al., 2013) cannot be applied in the context of the ECA, because the cubic function assumes the speed is constant over a voyage, which is not the case once the voyage crosses the ECA. This study incorporates changes in the fuel function to yield a novel joint decision problem on fleet deployment and green technology adoption. The proposed model is very complex and contains several nonlinear components. We first use some techniques to linearize the nonlinear components except the fuel cost in objective function. A three-phase heuristic is then developed to solve the transformed model.

The remainder of this study is organized as follows. An overview of the related works is introduced in Section 2. Section 3 proposes a nonlinear MIP model to determine an optimal fleet deployment together with green technology adoption. A three-phase heuristic is developed in Section 4. Section 5 reports the computational experiments with real-world data. Conclusions are outlined in the last section.

2. Literature review and discussion

Although this study considers green technology adoption, the core part of the decision is still related to the widely studied fleet deployment problems. Readers who are interested in broader surveys can refer to Ronen (1993), Christiansen et al. (2004, 2013), Meng et al. (2013), Fransoo and Lee (2013) and Lee and Song (2017) for a comprehensive overview of fleet deployment problems.

Most of existing studies focus on determining the suitable size of ships deployed on each route. Xia et al. (2015) proposed a comprehensive model on fleet deployment considering the cargo allocation in a network and speed optimization. While this study further considers the decision on green technology adoption in fleets, the penalty on the delivery delay of cargos, transshipment cost in the network, and some extra cost related to shore power. Psaraftis (2016) introduced the quest for win-win solutions in green transportation logistics. Zis and Psaraftis (2017) proposed a modal split model to estimate modal shifts between competing maritime and land-based modes available for shippers without the consideration of green technologies, and pointed out that installing green technologies for shipping companies are among the measures that should be considered in future studies, which means that retrofitting existing fleets, such as the number of ships newly equipped different green technologies, is critical for shipping companies to comply with stricter global fuel emission regulations. The main contribution of our study is to put the fleet deployment problem in the background of the green shipping, which has currently received significant attention from both academia and industry (Fagerholt et al., 2015). These green shipping studies mainly focus on air pollution, sewage pollution, and greenhouse gas emissions (Corbett et al., 2009; Cariou, 2011; Lai et al., 2011). However, our study focuses on technology adoption in green shipping. Thus, the following paragraphs mainly review the related works through two streams: one is about green technology adoption in the generic maritime industry, the other is about the adoption of green technologies for some specific ship routes.

In the area of green technology adoption in maritime industry, Yang et al. (2012) proposed a subjective generic methodology, as a transparent evaluation tool for ship owners, to select their preferred emissions control techniques. Brynolf et al. (2014) evaluated SO_X and NO_X compliance possibilities among three alternative reduction options (MGO, scrubbers, and liquefied natural gas) for the future ECA. Ren and Lützen (2015) developed a multi-criteria decision-making methodology to help shipping companies select emissions reduction technologies. In the real world, some shipping companies, such as Maersk and Wallenius Wilhelmsen ASA, have shown an environmentally proactive attitude towards green shipping, especially emissions reduction, and have taken the lead in the development and exploitation of emission reduction methods (Acciaro, 2014). Atari and Prause (2017) investigated the evaluation of scrubbers, determined the best investment opportunity and the decision with highest return among two compliance methods (fuel switching and scrubber installation). The MIP model proposed by Zhen et al. (2018) can save fuel costs under ECA regulations. It is therefore obvious that the technical options to comply with the ECA regulations are becoming increasingly important.

For some specific ship routes, studies on green technology adoption were also conducted. Jiang et al. (2014) examined the costs and benefits of a typical container ship travelling between Rotterdam (Netherlands) and Gothenburg (Sweden) after applying different green technologies. Armellini et al. (2018) analyzed different solutions (burning HFO and installing scrubbers, burning MGO) by using real data from a real cruise ship sailing between Barcelona (Spain) and Venice (Italy). Patricksson et al. (2015) proposed a mathematical model for a fleet renewal problem faced by the liner shipping company Wallenius Wilhelmsen Logistics in the context of ECAs, but they only considered scrubbers without mentioning other green technologies. Ölçer and Ballini (2015) proposed a decision-making framework for the evaluation of different green technologies, which facilitates the inclusion of all combinations of decision-making parameters and focuses on the port of Copenhagen. Hence, we note that some studies focus on the evaluation of different green technologies on a given ship route or area, but few studies can provide a quantitative decision methodology on the green technology adoption for fleet deployment on a shipping network in the context of ECAs.

In summary, the majority of the existing studies on ECA regulations have not used quantitative methodologies. A few studies do, but they do not incorporate sulphur reduction within fleet deployment decisions and apply their methods to a shipping network. However, it is essential to consider the emission reduction for fleet deployment of a shipping network in the context of ECAs. Both of the above-mentioned problems (green technology adoption, fleet deployment) belong to strategical decisions, which have a long-term influence on shipping companies' operations and development. Therefore, this paper connects fleet deployment and green technology adoption. More specifically, we also consider how to meet the container shipping demand of origin-destination (OD) pairs. Moreover, some other operating limits, such as the availability of berths and transit time requirements, have also been frequently ignored in previous studies, even though these factors are crucial to the real-world seaborne activities. Our paper takes into account these realistic factors in model formulation and algorithm design.

We formulate an integrated decision model which incorporates technology adoption, fleet deployment, service scheduling, and cargo allocation decisions under ECA regulations. Several realistic factors, such as transshipment activities, port resources, and transit time requirements are incorporated in the model. These features make this paper significantly different from previous studies.

3. Model formulation

We consider a general service network containing a set R of container ship routes (services), which consists of a set P of ports. Figure 1 depicts a shipping network with four routes and nine physical ports. For each ship route r, let I_r represent the set of ports of call (legs), ship route r having $|I_r|$ ports of call. Each ship route $r \in R$ is described as (port p_{r1}, port $p_{r2}, \cdots$, port $p_{ri}, \cdots$, port $p_{r|I_r|}$, port p_{r1}). We denote by leg i the voyage from port p_{ri} to port $p_{r,i+1}$, where $p_{r,|I_r|+1} = p_{r1}$. Let pair $< r, i >$ denote leg i of ship route r. The objective and constraints considered in this study are introduced in the following subsections.

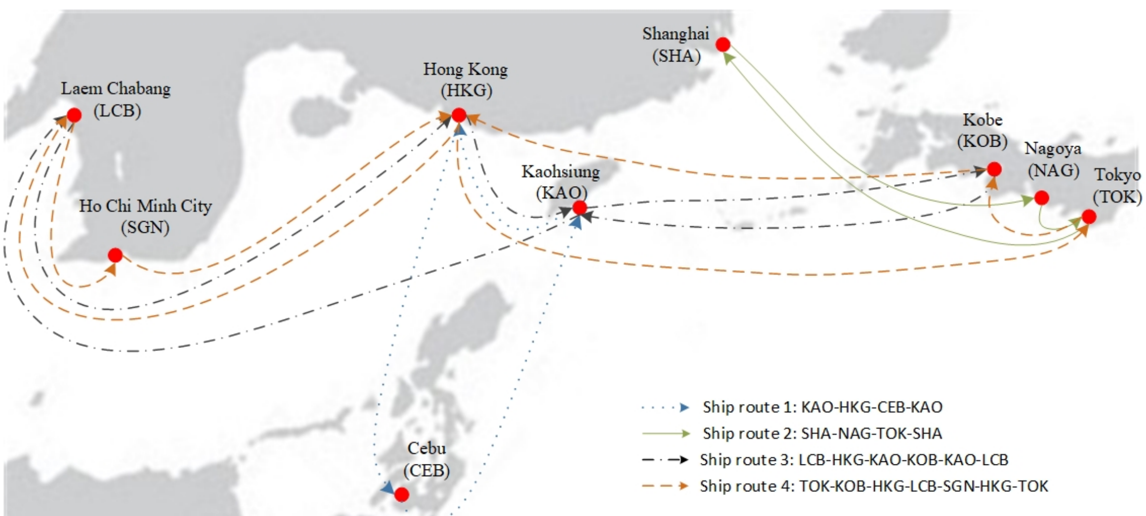

Figure 1: A shipping network with four routes

3.1. Initial investment and operating costs of ships

A fleet of ships is deployed on each route r in a service network and maintains a weekly service frequency. This study considers two green technologies when retrofitting ships. The first technology is scrubbers, and the second technology is shore power. Hence, four types of ships (ships with only scrubbers, ships with only shore power, ships with scrubbers and shore power, and ships without scrubbers or shore power) can be deployed on each route. The numbers of such ships on route r are denoted by β_r^S, β_r^P, β_r^{SP} and β_r^{ϕ}, respectively. The initial investment cost for all ships on all routes during one week can be calculated as $\sum_{r\in R} m_r^S(\beta_r^{SP}+\beta_r^S) + m_r^P(\beta_r^{SP}+\beta_r^P)$, where m_r^S and m_r^P are the weekly costs for installing scrubbers and shore power, respectively, for a ship on route r. Moreover, the total weekly operating cost for all deployed ships on all routes during one week can be calculated as $\sum_{r\in R}(c_r^{SP}\beta_r^{SP} + c_r^S\beta_r^S + c_r^P\beta_r^P + c_r^{\phi}\beta_r^{\phi})$, where c_r^{SP}, c_r^S, c_r^P and c_r^{ϕ} are the weekly operating cost for deploying one ship with scrubbers and shore power, one ship with only scrubbers, one ship with only shore power, and one ship without scrubbers or shore power, respectively, on route r. It is usual practice in related studies on liner shipping networks to consider the fixed cost of ships as weekly cost in the models' objectives (Du et al., 2016; Brouer et al., 2017).

It should be noted that a scrubber can reduce a ship's sulphur emission to below either 0.5% or 0.1% (Plakantonaki, 2017). Hence, this study assumes the fixed cost for installing the scrubber on a ship travelling within ECAs with sulphur limit of 0.1% or 0.5% is the same. In addition, the above definition on the weekly based investment and operating cost lies on an implicit assumption that the usage time of scrubbers is deterministic. If there is uncertainty in the equipment usage time, there actually exists a potential benefit for the way of using clean fuel by comparing with the way of installing equipment. For the sake of simplicity, the potential benefit on the flexibility of using clean fuel under uncertain environment is not considered in our objective. In a further study considering uncertainty, this issue could be taken into account on the basis of the model we propose.

3.2. Fuel cost

For the shipping companies, the fuel cost accounts for more than 50% of the total operating costs (Fagerholt and Psaraftis, 2015). Hence, the fuel cost should be a very important part in shipping. Let $f_{ri}^1(\gamma_{ri})$ and $f_{ri}^2(\gamma_{ri})$ represent the fuel cost of leg $< r, i >$ with sailing time γ_{ri} if ships do not have scrubbers, and the fuel cost if ships are equipped with scrubbers, respectively. From a related working paper (Wang et al., 2019), we know that two cases for calculating $f_{ri}^1(\gamma_{ri})$ should be considered. If leg i

of route r covers ECAs, we have:

$$f_{ri}^1(\gamma_{ri}) = \begin{cases} a(\gamma_{ri} - T_{ri}^0)^{-b}\alpha_E (L_{ri}^E)^{b+1} + a(T_{ri}^0)^{-b}\alpha_N (L_{ri}^N)^{b+1} & T_{ri}^{'} \leq \gamma_{ri} < \hat{T}_{ri} \\ a\gamma_{ri}^{-b}(\alpha_E^{\frac{1}{b+1}} L_{ri}^E + \alpha_N^{\frac{1}{b+1}} L_{ri}^N)^{b+1} & \gamma_{ri} > \hat{T}_{ri} \end{cases} \tag{1}$$

$$f_{ri}^2(\gamma_{ri}) = \alpha_N (L_{ri}^E + L_{ri}^N) a (\frac{L_{ri}^E + L_{ri}^N}{\gamma_{ri}})^b = a\gamma_{ri}^{-b}\alpha_N (L_{ri}^E + L_{ri}^N)^{b+1}, \tag{2}$$

and if leg i of route r does not cover ECAs, we have:

$$f_{ri}^1(\gamma_{ri}) = f_{ri}^2(\gamma_{ri}) = \alpha_N (L_{ri}^E + L_{ri}^N) a (\frac{L_{ri}^E + L_{ri}^N}{\gamma_{ri}})^b = a\gamma_{ri}^{-b}\alpha_N (L_{ri}^E + L_{ri}^N)^{b+1}, \tag{3}$$

where $T_{ri}^0 := \frac{L_{ri}^N}{\bar{e}_{ri}}$, $T_{ri}^{'} := \frac{L_{ri}^E + L_{ri}^N}{\bar{e}_{ri}}$, $\hat{T}_{ri} := \frac{\alpha_E^{\frac{1}{b+1}} L_{ri}^E + \alpha_N^{\frac{1}{b+1}} L_{ri}^N}{\alpha_N^{\frac{1}{b+1}} \bar{e}_{ri}}$. The sailing distance within the ECA of leg i on the route r is L_{ri}^E, and the distance outside the ECA is L_{ri}^N. Let $\bar{e}_{ri}$ denote maximum speeds of ships traveling on the i^{th} leg on ship route r. The letters a and b represent conversion factors between fuel consumption per unit distance and sailing speed: fuel consumption per unit distance is $a \cdot (\frac{L_{ri}^E + L_{ri}^N}{\gamma_{ri}})^b$ (ton/nautical mile). α_E and α_N denote unit price (USD/ton) of MGO and HFO, respectively. Let γ_{ri} represent the sailing time of the leg $< r, i >$. We denote by h_r the number of ships deployed on route r. Hence, the total fuel cost is calculated as $\sum_{r \in R} \sum_{i \in I_r} [\frac{\beta_r^P + \beta_r^{\phi}}{h_r} f_{ri}^1(\gamma_{ri}) + \frac{\beta_r^{SP} + \beta_r^S}{h_r} f_{ri}^2(\gamma_{ri})]$.

3.3. Transshipment cost

Since our problem arises in the context of a shipping network, the cost for transshipping cargos should also be taken into account. The transshipment cost is calculated on the basis of a concept called "transportation plan", which was used in some related works on ship deployment (Zhen et al., 2019b). More specifically, for each OD pair of transportation demand (e.g., the containers need to be transported from port p to port q), we define a set Y_{pq} of transportation plans y. According to the planners' experience and realistic factors, the set of transportation plans for each OD pair can be predefined. For ease of understanding, Figure 1 shows an example with four routes in a shipping network, and some transportation plans can be defined in Table 1. For example, if some containers need to be transported from port HKG to port KAO, they can be shipped directly, or they can be shipped from port HKG to port GES then to port KAO.

Table 1: Example of some transportation plans for container routing

OD		Transportation plans
HKG-KAO	$y_1 \in Y_{HKG,KAO}$	$< p_{r_1,2}, p_{r_1,3} > + < p_{r_1,3}, p_{r_1,1} >$
	$y_2 \in Y_{HKG,KAO}$	$< p_{r_3,2}, p_{r_3,3} >$
LCB-HKG	$y_3 \in Y_{LCB,HKG}$	$< p_{r_3,1}, p_{r_3,2} >$
	$y_4 \in Y_{LCB,HKG}$	$< p_{r_4,4}, p_{r_4,5} > + < p_{r_4,5}, p_{r_4,6} >$

Based on the defined set of transportation plans for each OD pair (e.g., the set Y_{pq} for OD pair (p, q)), the container routing decision is to allocate the containers of the OD pair (the number of the containers is defined as n_{pq}) among all transportation plans in the set Y_{pq}. We define by π_y the number of containers transported by plan y, $\sum_{y \in Y_{pq}} \pi_y = n_{pq}$.

Some containers on an OD pair may be delivered through transshipment (Bell et al., 2013). To transport containers from their origins to their destinations, it is easy to understand that the most suitable way is direct shipping. However, due to either the limitation of ship volume capacity or if there is no direct ship route for the OD pair, direct shipping often does not happen. The main cost of transshipment is the handling cost. Since each transportation plan's route is deterministic, the number of transshipment activities (unloading and loading) for each container is also known. Let c_y^T denote the unit transshipment handling cost associated with transportation plan y. Then the total handling cost for transshipped containers is calculated as: $\sum_{p \in P} \sum_{q \in P} \sum_{y \in Y_{pq}} c_y^T \pi_y$.

3.4. Service level related penalty

The service level of an OD pair is related to the actual delivery time of containers. For each OD pair $< p, q >$, there is a normal transportation time T_{pq} in the seaborne shipping market. A penalty cost should be paid if the actual delivery time τ_y of a container needing to be shipped from port p to port q is longer than T_{pq}. Let c_{pq}^D define the unit penalty cost, then the value of the penalty cost of the delayed container for OD pair $< p,q >$ is computed as $c_{pq}^D(\tau_y - T_{pq})^+$, where $(x)^+ = \max\{0, x\}$. The value of $\sum_{p\in P}\sum_{q\in P}\sum_{y\in Y_{pq}} \pi_y c_{pq}^D(\tau_y - T_{pq})^+$ is the total penalty cost for all shipped containers. Here τ_y represents the actual total time of fulfilling transportation plan y, which consists of the ship sailing time, the ship dwelling time at the ports, and the waiting time when the containers are transshipped at the ports. It can be computed as $\tau_y = \sum_{r\in R}\sum_{i\in I_r} k_{yri}\gamma_{ri} + \sum_{r\in R}\sum_{i\in I_r} k_{yri}d_{ri} + \sum_{<r,i,s,j>\in Q} k_{yrisj}\delta_{risj}$ where k_{yri} is a binary parameter equal to one if and only if plan y uses leg $< r,i >$. The parameter d_{ri} represents dwell duration of a ship at the i^{th} port of call on ship route r. The binary parameter k_{yrisj} equals to one if and only if plan y uses the $< r,i,s,j >$, which denotes that containers shipped through plan y will be transshipped from the i^{th} port of call on ship route r to the j^{th} port of call on ship route s.

3.5. Extra cost for ships with shore power using berths without shore power

Each port usually reserves a limited number of berths with shore power for a shipping liner. Extra costs are incurred if more berths with shore power are needed by the shipping liner (Zhen et al., 2019a). In this study, let B_p represent the set of berths equipped with shore power b in port p booked for the shipping liner. The index $\hat{b}$ is defined as a dummy berth, which is used when there are no available berths with shore power in the booked berth set B_p when a ship arrives at port p. From the perspective of modeling, if the dummy berth $\hat{b}$ is used by a ship with shore power, then an extra cost is incurred. Here, we define binary decision variable λ_{rib} to denote whether the ship arrives at berth with shore power b in the leg $< r,i >$, and we define c_p^B as the penalty cost incurred when the dummy berth $\hat{b}$ is used in the leg $< r,i >$. Then the total cost for extra berth usage is $\sum_{r\in R}\sum_{i\in I_r} \frac{\beta_r^{SP}+\beta_r^P}{h_r} c_p^B \lambda_{ri\hat{b}}$.

It should be noted that not all berths have a high-voltage shore connection system. According to the Innes and Monios (2018), there were only 28 ports in the world with shore power installed at the end of 2017. By February 2018, the installation rate of shore power in the berths of Shanghai port (China) was only about 10% (IOoSM, 2018). Hence, it is realistic and common that not all berths have a high-voltage shore connection system. And the berth allocation should be a decision of the optimization model.

3.6. Mathematical model formulation

Based on the above analysis on the components of objective values, we formulate a nonlinear model. We make the following assumptions:

(1) The shipping network of the ports and routes (voyages) is already determined.

(2) The ships on each route are homogenous in terms of capacity.

(3) The volume of container transportation demands for each OD is known in advance. These data can be estimated from historical records (Fagerholt et al., 2009; Bell et al., 2011).

(4) The ships' dwell time at each port of call is deterministic.

(5) The usage time of scrubbers is deterministic.

(6) Not all berths have a power shore connection system.

Before formulating the mathematical model for this problem, we list the notations used in this paper as follows.

Indices and sets

r (or s)	index of a ship route, $r \in R$.
R	set of all ship routes.
i (or j)	index of port of call (or leg) on a ship route (leg i is from port of call i to i+1).
I_r	set of the ports of call (or legs) on ship route r.
$\langle r, i, s, j \rangle$	a transshipment from the i^{th} port of call on ship route r to the j^{th} port of call on ship route s ; $r, s \in R$; $i \in I_r$, $j \in I_s$. A quadruple $< r, i, s, j >$ means that the i^{th} port of call on ship route r and the j^{th} port of call on ship route s correspond to the same physical port in the network, i.e., $p_{ri} = p_{sj}$.
Q	set of quadruples $< r, i, s, j >$; $Q = \{< r, i, s, j > \| p_{ri} = p_{sj}\}$.
p (or q)	index of a physical port, which is different from the "port of call" (defined as i) on a ship route, $p \in P$.

316 P set of all the ports.

317 p_{ri} index of the port that corresponds to the i^{th} port of call on ship route r, $p_{ri} \in P$.

318 y index of a transportation plan for fulfilling the transportation task of an OD pair.

319 Y_{pq} set of transportation plans for shipping containers from port p to port q; $p, q \in P$.

320 w index of a day in a week, i.e., 0 = Sun, 1 = Mon, 2 = Tue,$\cdots$, 6 = Sat.

321 W set of days in a week, $W = \{0, 1, 2, \cdots, 6\}$.

322 b index of a berth.

323 B_p set of berths with shore power in port p that are reserved for the shipping liner.

324 $\hat{b}$ index of a dummy berth, which is used when there are no available berths with shore power in the reserved berth set B_p when a ship arrives at port p.

325 I'_{rp} set of the ports of call (or legs) on ship route r that correspond to the same physical port p.

326 R'_p set of the ship routes that include port p.

327 $\mathbb{Z}$ set of integers.

328 $\mathbb{Z}_+$ set of non-negative integers.

329 **Parameters**

330 c_r^S weekly operating cost of a ship with only scrubbers deployed on ship route r.

331 c_r^P weekly operating cost of a ship with only shore power deployed on ship route r.

332 c_r^{ϕ} weekly operating cost of a ship without scrubbers or shore power deployed on ship route r.

333 c_r^{SP} weekly operating cost of a ship with scrubbers and shore power deployed on ship route r.

334 h_r number of ships deployed on ship route r.

335 α_E unit price (USD/ton) of MGO.

336 α_N unit price (USD/ton) of HFO.

337 a, b conversion factors between fuel consumption per unit distance and sailing speed.

338 $f_{ri}^1(\gamma_{ri})$ fuel cost of leg $< r, i >$ with sailing time γ_{ri} if the ship sailing on the leg does not have scrubbers.

339 $f_{ri}^2(\gamma_{ri})$ fuel cost of leg $< r, i >$ with sailing time γ_{ri} if the ship sailing on the leg has scrubbers.

340 m_r^S weekly cost for installing scrubbers for a ship on ship route r.

341 m_r^P weekly cost for installing shore power for a ship on ship route r.

342 c_y^T unit transshipment cost (USD per twenty-foot equivalent unit, USD/TEU) for handling containers when transshipped in transportation plan y.

343 n_{pq} number of containers (TEUs) that need to be transported from port p to port q each week. This value can be estimated from historical data.

344 T_{pq} normal number of days for containers to be transported from port p to port q.

345 v_r volume capacity (TEUs) of each ship deployed on ship route r.

346 L_{ri}^E sailing distance for leg i on route r within ECAs.

347 L_{ri}^N sailing distance for leg i on route r outside ECAs.

348 d_{ri} dwell duration (days) of a ship at the i^{th} port of call on ship route r.

D_r total dwell duration (days) of a ship on ship route r.

$\bar{D}$ maximum value of dwell duration for all the ports of call (days), $\bar{D}$ =max$\{d_{ri}, r \in R, i \in I_r\}$.

c_p^B extra cost for a ship with shore power mooring at a berth without shore power. It is used as the penalty cost each time the dummy berth $\hat{b}$ is used at the port p.

c_{pq}^D unit penalty cost (USD per TEU per day) for the delay of delivering containers from port p to port q.

k_{yrisj} equal to one if and only if plan y uses transshipment $< r, i, s, j >$; and zero otherwise.

k_{yri} equal to one if and only if plan y uses the i^{th} leg on ship route r (or visits the i^{th} port of call on ship route r), and zero otherwise.

g_{bw} equal to one if and only if berth b is available on the day w in a week, and zero otherwise.

$\overline{e}_{ri}, \underline{e}_{ri}$ maximum and minimum speeds of ships traveling on the i^{th} leg on ship route r, respectively.

$[\theta_{ri}^{min}, \theta_{ri}^{max}]$ arrival time window at the i^{th} port of call on ship route r in a week; due to the weekly service frequency, we have $\theta_{ri} \in [\theta_{ri}^{min}, \theta_{ri}^{max}] \cup [\theta_{ri}^{min} + 7, \theta_{ri}^{max} + 7] \cup [\theta_{ri}^{min} + 14, \theta_{ri}^{max} + 14] \cdots$.

Variables

(1) Ship deployment decision:

β_r^{SP} number of ships with both scrubbers and shore power deployed on route r.

β_r^S number of ships with only scrubbers deployed on route r.

β_r^P number of ships with only shore power deployed on route r.

β_r^{ϕ} number of ships without scrubbers or shore power deployed on route r.

(2) Timing decision (service schedule):

365 θ_{ri} — time (day) at which a ship arrives at the i^{th} port of call on ship route r. Here $\theta_{ri} \in \mathbb{Z}_+; i = 1, 2, \cdots, |I_r|, |I_r| + 1$; without loss of generality, we require $\theta_{r1} \in \{0, 1, 2, \cdots, 6\}$; $\theta_{r,|I_r|+1}$ denotes the time (day) when the ship returns to the first port of call on ship route r, i.e., $\theta_{r,|I_r|+1}$ is equal to θ_{r1}, plus the number of days required by a ship to complete a round trip journey.

366 **(3) Ship speed decision:**

367 γ_{ri} — sailing time (days) of the i^{th} leg on ship route r. It actually reflects the ship sailing speed decision on each leg in the network.

368 **(4) Container routing decision:**

369 π_y — number of containers (TEUs) shipped through transportation plan y.

370 **(5) Berth allocation decision:**

371 λ_{rib} — set to one if and only if the ship uses the berth b (including $\hat{b}$) on leg $< r, i >$, and zero otherwise.

372 **(6) Auxiliary decisions:**

373 τ_y — duration (days) for fulfilling plan y, including the voyage time on sea (sailing and dwelling at berth), and the containers' waiting time at yard for transshipment.

374 δ_{risj} — the value of arrival time difference (days) of a ship that visits $< r, i >$ and a ship that visits $< s, j >$ mod 7; $\delta_{risj} \in \{0, 1, \cdots, 6\}$.

375 ξ_{risj} — an integer associated to variable δ_{risj}. It is used to transfer the difference of arrival day θ_{ri} and θ_{sj} to a non-negative integer of the seven days, which is denoted by δ_{risj}.

376 η_{riw} — set to one if and only if the ship arrives at the ports of call $< r, i >$ on the day w of a week, and zero otherwise.

377 ζ_{ri} — auxiliary variable associated with θ_{ri} to transfer the θ_{ri} to a day in one week.

378 **Mathematical model**

379 Based on the above definitions of parameters and variables, we formulate a non-

linear mathematical model as follows:

$$[\boldsymbol{M1}] \quad \text{Minimize Z} = \underbrace{\sum_{r \in R}[m_r^S(\beta_r^{SP} + \beta_r^S) + m_r^P(\beta_r^{SP} + \beta_r^P) + c_r^{SP}\beta_r^{SP} + c_r^S\beta_r^S + c_r^P\beta_r^P + c_r^\phi\beta_r^\phi]}_{\textit{initial investment and operating cost of ships}}$$
$$+ \underbrace{\sum_{r \in R}\sum_{i \in I_r}[\frac{\beta_r^P + \beta_r^\phi}{h_r} f_{ri}^1(\gamma_{ri}) + \frac{\beta_r^{SP} + \beta_r^S}{h_r} f_{ri}^2(\gamma_{ri})]}_{\textit{fuel cost}} + \underbrace{\sum_{p \in P}\sum_{q \in P}\sum_{y \in Y_{pq}} c_y^T \pi_y}_{\textit{transshipment cost}}$$
$$+ \underbrace{\sum_{p \in P}\sum_{q \in P}\sum_{y \in Y_{pq}} \pi_y c_{pq}^D(\tau_y - T_{pq})^+}_{\textit{service level related penalty}} + \underbrace{\sum_{r \in R}\sum_{i \in I_r} \frac{\beta_r^{SP} + \beta_r^P}{h_r} c_p^B \lambda_{ri\hat{b}}}_{\textit{extra cost for berths without shore power}} \tag{4}$$

subject to

$$\tau_y = \sum_{r \in R}\sum_{i \in I_r} k_{yri}\gamma_{ri} + \sum_{r \in R}\sum_{i \in I_r} k_{yri}d_{ri} + \sum_{<r,i,s,j> \in Q} k_{yrisj}\delta_{risj} \quad \forall p \in P, q \in P, y \in Y_{pq} \tag{5}$$

$$\beta_r^{SP} + \beta_r^S + \beta_r^P + \beta_r^\phi = h_r \quad \forall r \in R \tag{6}$$

$$0 \;\leq\; \theta_{r1} \;\leq\; 6 \quad \forall r \in R \tag{7}$$

$$\left\lceil \frac{L_{ri}^E + L_{ri}^N}{\overline{e}_{ri}} \right\rceil \;\leq\; \gamma_{ri} \;\leq\; \left\lfloor \frac{L_{ri}^E + L_{ri}^N}{\underline{e}_{ri}} \right\rfloor \quad \forall r \in R, i \in I_r \tag{8}$$

$$\theta_{r,i+1} = \theta_{ri} + d_{ri} + \gamma_{ri} \quad \forall r \in R, i \in I_r \tag{9}$$

$$\theta_{r,|I_r|+1} = \theta_{r1} + 7h_r \quad \forall r \in R \tag{10}$$

$$\theta_{sj} - \theta_{ri} + 7\xi_{risj} = \delta_{risj} \quad \forall <r,i,s,j> \in Q \tag{11}$$

$$0 \;\leq\; \delta_{risj} \leq 6 \quad \forall <r,i,s,j> \in Q \tag{12}$$

$$-h_s \;\leq\; \xi_{risj} \leq h_r \quad \forall <r,i,s,j> \in Q \tag{13}$$

$$\sum_{y \in Y_{pq}} \pi_y = n_{pq} \quad \forall p \in P, q \in P \tag{14}$$

$$\sum_{p \in P} \sum_{q \in P} \sum_{y \in Y_{pq}} k_{yri} \pi_y \ \leq \ v_r \quad \forall r \in R, i \in I_r \tag{15}$$

$$\sum_{w \in W} \eta_{riw} = 1 \quad \forall r \in R, i \in I_r \tag{16}$$

$$\theta_{ri} = \sum_{w \in W} w \eta_{riw} + 7\zeta_{ri} \quad \forall r \in R, i \in I_r \tag{17}$$

$$0 \ \leq \ \zeta_{ri} \ \leq \ h_r - 1 \quad \forall r \in R, i \in I_r \tag{18}$$

$$\sum_{b \in B_p \cup \{\hat{b}\}} \lambda_{rib} = 1 \quad \forall r \in R, i \in I_r \tag{19}$$

$$\sum_{r \in R'_p} \sum_{i \in I'_{rp}} \sum_{k=0}^{d_{ri}-1} \lambda_{rib} \eta_{r,i,(w-k) \bmod 7} \ \leq \ g_{bw} \quad \forall p \in P, b \in B_p, w \in W \tag{20}$$

$$\theta_{r1}^{min} \ \leq \ \theta_{r1} \leq \theta_{r1}^{max} \quad \forall r \in R \tag{21}$$

$$\theta_{ri}^{min} \ \leq \ \sum_{w \in W} w \eta_{riw} \leq \theta_{ri}^{max} \quad \forall r \in R, i \in I_r \tag{22}$$

$$\beta_r^{SP}, \beta_r^{S}, \beta_r^{P}, \beta_r^{\phi} \in \mathbb{Z}_+ \quad \forall r \in R \tag{23}$$

$$\gamma_{ri}, \theta_{ri}, \zeta_{ri}, \delta_{ri} \in \mathbb{Z}_+ \quad \forall r \in R, i \in I_r \tag{24}$$

$$\pi_y, \tau_y \in \mathbb{Z}_+ \quad \forall p \in P, q \in P, y \in Y_{pq} \tag{25}$$

$$\lambda_{rib} \in \{0, 1\} \quad \forall r \in R, i \in I_r, b \in B_p \cup \{\hat{b}\} \tag{26}$$

$$\xi_{risj} \in \mathbb{Z} \quad \forall < r, i, s, j > \in Q \tag{27}$$

$$\eta_{riw} \in \{0, 1\} \quad r \in R, i \in I_r, w \in W. \tag{28}$$

The objective (4) minimizes the sum of the five types of cost: initial investment and operating cost of ships, fuel cost, transshipment cost, service level related penalty cost, and extra cost for berths without shore power. The objective integrates some long-term and short-term decisions, which follows common practice of mode formulation in the fields of liner shipping network (Song and Dong, 2013; Karsten et al., 2017; Lin and Chang, 2018) and widely studied supply chain network (Zhang et al., 2014; Üster and Hwang, 2016). Constraints (5) calculate the value of τ_y, which includes the sailing time, the dwell time at a berth, and the transshipment handling time. Constraints (6) calculate the number of the four types of ships deployed on each route. Constraints (7) guarantee that the ship deployed on a route visits the first port within the first week of the planning horizon, which actually implies that all the liner services follow the weekly pattern. Constraints (8) define the range of the sailing time on each leg, which actually sets the limitation on the sailing speed during each leg. Constraints (9) link the arrival time θ_{ri} of a port of call with the arrival time $\theta_{r,i+1}$ of the next port of call on a route. Constraints (10) ensure that the total number of days for a ship completing its travel on a route $\theta_{r,|I_r|+1} - \theta_{r1}$ is the number of ships deployed on the route times seven, because all the services follow weekly arrival pattern and one week contains seven days. Constraints (11)–(13) compute the arrival time difference between the ports of call $< r, i >$ and $< s, j >$ at a transshipment port $< r, i, s, j >$. Constraints (14) calculate the number of containers with the same OD pair. Constraints (15) guarantee that the number of containers carried by each ship on a route does not exceed the ship capacity. Constraints (16)–(18) connect the binary variable η_{riw} and the integer variable θ_{ri}, both of which denote the arrival time at the i^{th} port of call on ship route r. The difference is that θ_{ri} denotes the arrival time on a universal time axis, while η_{riw} denotes the arrival time on one of the seven days in a week. The former is from the perspective of port arrival time in one ship's itinerary (e.g., day 3 at port 1, day 13 at port 2), while the latter is from the perspective of the port arrival time of a fleet of ships deployed on a route (e.g., Wed. at port 1, Sat. at port 2). Constraints (19) ensure that each port of call of a route should be assigned a berth (one of reserved berths or the dummy berth $\hat{b}$). Constraints (20) enforce the berth availability limitation. Constraints (21)–(22) ensure that the arrival time at the i^{th} port of call on ship route r does not exceed its corresponding arrival time window. Constraints (23)–(28) state the ranges of the decision variables.

It is obvious that the proposed model [M1] is nonlinear. The first nonlinear part is the function of fuel cost in objective function (4), $\sum_{r\in R}\sum_{i\in I_r}[\frac{\beta_r^P+\beta_r^\phi}{h_r}f_{ri}^1(\gamma_{ri}) + \frac{\beta_r^{SP}+\beta_r^S}{h_r}f_{ri}^2(\gamma_{ri})]$. The function of extra cost for berths without shore power in objective function (4) is also nonlinear. To be specific, the penalty cost $\sum_{r \in R} \sum_{i \in I_r} \frac{\beta_r^{SP} + \beta_r^P}{h_r} c_p^B \lambda_{ri\hat{b}}$ contains the product of variable $(\beta_r^{SP} + \beta_r^P)$ with variable $\lambda_{ri\hat{b}}$. The service level related penalty cost in the objective function (4) $\sum_{p \in P} \sum_{q \in P} \sum_{y \in Y_{pq}} \pi_y c_{pq}^D (\tau_y - T_{pq})^+$ contains the product of variable π_y with variable $(\tau_y - T_{pq})^+$. Moreover, the form $(\cdot)^+$ is also nonlinear. Finally, Constraints (20) contain a nonlinear part $\lambda_{rib} \eta_{r,i,(w-k) \bmod 7}$, which is the product of two binary variables. In order to speed up the solution process, we will first linearize the nonlinear functions of [M1] except the fuel cost nonlinear part in objective function (54) to form model [M2], which is summarized in Appendix 2. Then we propose a three-phase heuristic to solve this model, which is explained in the next section. We also linearize the whole nonlinear functions of [M1] to form model [M3], which is summarized in Appendix 3.

4. Three-phase heuristic

It is challenging to solve the nonlinear model [M2], which contains much more complex fuel cost functions than those used in traditional liner shipping related models. By reviewing the algorithms as well as their features in some existing fleet deployment studies, we found that specially tailored solution methods were usually developed to solve the models. There seems to be no commonly used (or widely employed) methodology in algorithm design for the fleet deployment decision models. For example, Agarwal and Ergun (2008) implement three heuristics (a greedy heuristic, a column generation based algorithm, and a Benders decomposition based algorithm) for a ship scheduling and network design problem in liner shipping. Meng et al. (2012) apply an algorithm integrating the sample average approximation with a dual decomposition and Lagrangian relaxation approach to solve a fleet deployment problem. Song and Dong (2013) propose a three-stage optimization method to tackle a service route design with ship deployment and empty container repositioning. Bakkehaug et al. (2016) design an adaptive large neighborhood search heuristic for a fleet deployment problem. Reinhardt et al. (2016) also show that bunker curves can be approximated by a number of linear secants. Even though fuel cost functions f_{ri}^1 and f_{ri}^2 in our model can be approximated by a number of linear secants, this study still need to multiply the linear fuel cost functions (including ship speed decision γ_{ri}) by ship deployment decisions (β_r^P, β_r^ϕ, β_r^{SP} and β_r^S). Hence, the whole part of fuel cost in the objective is still nonlinear. By considering the special structure and features of the model [M2], this study also designs a customised heuristic to solve the model.

The heuristic contains three phases. We propose in the first phase a fuel cost function transformation method based on dynamic programming. This method transfers fuel cost functions to some variables, which makes the proposed model [M2] tractable for CPLEX. However, for some large-scale instances, the transformed model remains difficult for CPLEX. Hence, the second phase of our heuristic is to decompose the model [M2] into two steps, i.e., solving the fleet deployment decisions first and then working with the remaining decision variables. The third phase improves the solution obtained by the previous two phases, by mainly considering the effect of berth allocation on the fleet deployment. The framework of our heuristic is outlined in Section 4.1, and some complex subprocesses are detailed in Sections 4.2 and 4.3.

4.1. Framework of the three-phase heuristic

The framework of the three-phase heuristic is shown in Algorithm 1. The three phases are introduced in the following three subsections.

Algorithm 1 Framework of the three-phase heuristic

Phase 1: fuel cost function transformation based on dynamic programming
for all the ship route $r, r \in R$ **do**
 for all the port of call $i, i \in I_r$ **do**
  Compute s_i // s_i is the total sailing time allocated to legs $i, i+1, ..., |I_r|$
  Compute $\Theta_{ri}(s_i)$ // $\Theta_{ri}(s_i)$ is the set of possible values of sailing time γ_{ri}
 end for
end for
for all the ship route $r, r \in R$ **do**
 $\beta_r^{SP}, \beta_r^{S}, \beta_r^{P}, \beta_r^{\phi} \leftarrow 0$
 while $\beta_r^{SP} \leqslant h_r$ **do**
  while $\beta_r^{S} \leqslant h_r$ **do**
   while $\beta_r^{P} \leqslant h_r$ **do**
    while $\beta_r^{\phi} \leqslant h_r$ **do**
     if $\beta_r^{SP} + \beta_r^{S} + \beta_r^{P} + \beta_r^{\phi} = h_r$ **then**
      Define $u_i(s_i, \gamma_{ri})$ // $u_i(s_i, \gamma_{ri})$ is the sum of fuel costs on legs $i, i+1, ..., |I_r|$ for each s_i and γ_{ri}
      Define $u_i^*(s_i)$ // $u_i^*(s_i)$ is the minimal value of $u_i(s_i, \gamma_{ri})$ under different values of γ_{ri}
      $i \leftarrow |I_r|$

$u_i^*(s_i) \leftarrow \frac{\beta_r^P + \beta_r^\phi}{h_r} f_{r,i}^1(s_i) + \frac{\beta_r^S + \beta_r^{SP}}{h_r} f_{r,i}^2(s_i)$
$i \leftarrow i - 1$
while $i \geq 1$ **do**
for all the sailing time $\gamma_{ri}, \gamma_{ri} \in \Theta_{ri}(s_i)$ $(s_i = s_{i+1} + \gamma_{ri})$ **do**
$u_i(s_i, \gamma_{ri}) \leftarrow \frac{\beta_r^P + \beta_r^\phi}{h_r} f_{r,i}^1(s_i) + \frac{\beta_r^S + \beta_r^{SP}}{h_r} f_{r,i}^2(s_i)$
end for
$u_i^*(s_i) \leftarrow \min_{\gamma_{ri} \in \Theta_{ri}(s_i)} u_i(s_i, \gamma_{ri})$
$i \leftarrow i - 1$
end while
$C_r(\beta_r^{SP}, \beta_r^S, \beta_r^P, \beta_r^\phi) \leftarrow u_1^*(s_1)$ //$C_r(\beta_r^{SP}, \beta_r^S, \beta_r^P, \beta_r^\phi)$ is the total fuel cost
else
$C_r(\beta_r^{SP}, \beta_r^S, \beta_r^P, \beta_r^\phi) \leftarrow \infty$
end if
$\beta_r^\phi \leftarrow \beta_r^\phi + 1$
end while
$\beta_r^P \leftarrow \beta_r^P + 1$
end while
$\beta_r^S \leftarrow \beta_r^S + 1$
end while
$\beta_r^{SP} \leftarrow \beta_r^{SP} + 1$
end while
end for
Phase 2: solving model by approximate division
Formulate the model [M4] by replacing "fuel cost" in [M2] with the above-mentioned "$C_r(\beta_r^{SP}, \beta_r^S, \beta_r^P, \beta_r^\phi)$" and removing the three types of costs (transshipment cost, service level related penalty, and extra cost for berths without shore power)
for all the ship route $r, r \in R$ **do**
Solve the model [M4] by CPLEX with given $\beta_r^{SP} = h_r, \beta_r^S = \beta_r^P = \beta_r^\phi = 0$
Solve the model [M4] by CPLEX with given $\beta_r^S = h_r, \beta_r^{SP} = \beta_r^P = \beta_r^\phi = 0$
Solve the model [M4] by CPLEX with given $\beta_r^P = h_r, \beta_r^S = \beta_r^{SP} = \beta_r^\phi = 0$
Solve the model [M4] by CPLEX with given $\beta_r^\phi = h_r, \beta_r^S = \beta_r^P = \beta_r^{SP} = 0$
// According to the Proposition 1 (elaborated in Section 4.3), each route has only one type of ship, so that only one β is positive, and other β are zero
Select the best solution $(\beta_r^{SP*}, \beta_r^{S*}, \beta_r^{P*}, \beta_r^{\phi*})$ which has the least objective value among the above four solutions
end for
Phase 3: solution improvement
Solve model [M2] (after fuel cost function transformation), similarly hereinafter, by CPLEX with given $\{\beta_r^{SP*}, \beta_r^{S*}, \beta_r^{P*}, \beta_r^{\phi*}, C_r(\beta_r^{SP}, \beta_r^S, \beta_r^P, \beta_r^\phi)_{r \in R}\}$
$d \leftarrow$ objective value // d counts the current objective value of model [M2]
for all the ship route $r, r \in R$ **do**

if $\beta_r^{P*} > 0$ **then**
$\beta_r^{P*} \leftarrow 0, \beta_r^{\phi*} \leftarrow h_r$
Solve model [M2] by CPLEX with given $\{\beta_r^{SP*}, \beta_r^{S*}, \beta_r^{P*}, \beta_r^{\phi*}, C_r(\beta_r^{SP}, \beta_r^{S}, \beta_r^{P}, \beta_r^{\phi})_{r\in R}\}$
$d1 \leftarrow$ objective value // $d1$ counts the current objective value of model [M2]
if $d1 > d$ **then**
$\beta_r^{P*} \leftarrow h_r, \beta_r^{\phi*} \leftarrow 0$
end if
else
if $\beta_r^{SP*} > 0$ **then**
$\beta_r^{SP*} \leftarrow 0, \beta_r^{S*} \leftarrow h_r$
Solve model [M2] by CPLEX with given $\{\beta_r^{SP*}, \beta_r^{S*}, \beta_r^{P*}, \beta_r^{\phi*}, C_r(\beta_r^{SP}, \beta_r^{S}, \beta_r^{P}, \beta_r^{\phi})_{r\in R}\}$
$d2 \leftarrow$ objective value // $d2$ counts the current objective value of model [M2]
if $d2 > d$ **then**
$\beta_r^{SP*} \leftarrow h_r, \beta_r^{S*} \leftarrow 0$
end if
end if
end if
end for
Solve model [M2] by CPLEX with given $\{\beta_r^{SP*}, \beta_r^{S*}, \beta_r^{P*}, \beta_r^{\phi*}, C_r(\beta_r^{SP}, \beta_r^{S}, \beta_r^{P}, \beta_r^{\phi})_{r\in R}\}$
Return the objective value and the values of the variables

4.1.1. Phase 1: Fuel cost function transformation

Phase 1 transfers the nonlinear fuel cost function in model [M2]. Because the decision variables γ_{ri} in the fuel cost function are the function arguments, model [M2] is nonlinear and cannot be solved by CPLEX directly. Hence, we derive in this phase a fuel cost function transformation method based on dynamic programming. To be specific, the fuel cost function is affected by the sailing speed on the legs, which is further determined by the fleet deployment. We enumerate all the feasible fleet deployment plans, denoted by $(\beta_r^{SP}, \beta_r^{S}, \beta_r^{P}, \beta_r^{\phi})$, which means that β_r^{SP} ships with scrubbers and shore power, β_r^{S} ships with only scrubbers, β_r^{P} ships with only shore power, and β_r^{ϕ} ships without scrubbers or shore power are deployed on route r. For each route, given the fleet deployment $(\beta_r^{SP}, \beta_r^{S}, \beta_r^{P}, \beta_r^{\phi})$, the speeds of legs are also enumerated within feasible ranges to calculate the minimum fuel cost denoted by $C_r(\beta_r^{SP}, \beta_r^{S}, \beta_r^{P}, \beta_r^{\phi})$. The enumeration process on the speeds of legs is implemented by dynamic programming, which is elaborated in Section 4.2. By replacing the fuel cost functions in the objective of model [M2] by the $C_r(\beta_r^{SP}, \beta_r^{S}, \beta_r^{P}, \beta_r^{\phi})$, the model becomes a mixed integer linear programming model, which may be solved by CPLEX for some small-scale instances.

4.1.2. Phase 2: Solving model by approximate division

Although model [M2] after the fuel cost function transformation may be tractable by CPLEX, it is still hard to solve for some large-scale instances. Therefore, Phase 2 computes an approximate solution by dividing the solution process of [M2] into two steps, i.e., solving the fleet deployment decisions first, and then solving the model for the remaining decision variables. The fleet deployment is independent of the transshipment cost and of the service level penalty, but is related to the initial investment cost, fixed operating cost of ships, fuel cost, and extra cost for berths without shore power. Among the costs affecting the fleet deployment, the influence of the extra cost for berths without shore power is relatively small. Hence, this phase assumes that all berths are equipped with shore power and ignores the influence of berth allocation. Based on the above assumption, we propose a simplified model [M4] which replaces the fuel cost in [M2] with the previously calculated $C_r(\beta_r^{SP}, \beta_r^S, \beta_r^P, \beta_r^\phi)$ and removes three types of cost (transshipment cost, service level related penalty, and extra cost for berths without shore power):

$$
\begin{aligned}
[\boldsymbol{M4}] \quad \underset{\beta_r^{SP},\beta_r^S,\beta_r^P,\beta_r^\phi,r=1,\cdots,|R|}{\text{Minimize}} \sum_{r\in R} [& m_r^S(\beta_r^{SP}+\beta_r^S) + m_r^P(\beta_r^{SP}+\beta_r^P) + c_r^{SP}\beta_r^{SP} + c_r^S\beta_r^S \\
& + c_r^P\beta_r^P + c_r^\phi\beta_r^\phi + C_r(\beta_r^{SP}, \beta_r^S, \beta_r^P, \beta_r^\phi)]
\end{aligned} \tag{29}
$$

subject to (6) and (23).

The allocation of the four types of ships to the routes can be determined by enumeration. However, we need not enumerate all possible combinations of fleet deployment $(\beta_r^{SP}, \beta_r^S, \beta_r^P, \beta_r^\phi) \in \{0,\cdots,h_r\} \times \{0,\cdots,h_r\} \times \{0,\cdots,h_r\} \times \{0,\cdots,h_r\}$ for each ship route r because Proposition 1, elaborated in Section 4.3, proves that each route has only one type of ship in an optimal plan for [M4]. This way, we only need to enumerate four possible combinations of fleet deployment for each ship route to determine the best fleet composition.

4.1.3. Phase 3: Solution improvement

Phase 3 improves the solution obtained by the previous two phases. After obtaining the fleet deployment $(\beta_r^{SP}, \beta_r^{S}, \beta_r^{P}, \beta_r^{\phi})$ (in Phase 2) and the values of $C_r(\beta_r^{SP}, \beta_r^{S}, \beta_r^{P}, \beta_r^{\phi})$, we solve model [M2] with CPLEX and we obtain a solution, which may contradict the assumption used to determine $(\beta_r^{SP}, \beta_r^{S}, \beta_r^{P}, \beta_r^{\phi})$ in Phase 2. More specifically, in Phase 2 we assumed that all berths are equipped with shore power to obtain the best fleet deployment scheduling. However, one route may be allocated ships with shore power (according to the solved solution in Phase 2) but these ships with shore power are moored at a berth without shore power (according to the solved solution in Phase 3). Hence, we should re-deploy the fleet by considering the effect of berth allocation on the fleet deployment. Because the benefits of scrubbers and of shore power are independent, there are three cases for the fleet deployment rescheduling process. (1) We do not need to reschedule the fleet deployment of route r if this route are allocated ships without shore power. (2) If the ships allocated to route r are only equipped with shore power, we should compare the cost of this condition with that of ships without scrubbers or shore power. (3) If the ships allocated to route r are equipped with shore power and scrubbers, we should compare the cost of this condition with that of ships with only scrubbers. After the above adjustments and rescheduling, we can obtain more realistic solutions.

4.2. Fuel cost function transformation based on dynamic programming

Because the decision variables γ_{ri} in the fuel cost function are the function arguments, model [M2] is intractable for CPLEX. Phase 1 transfers the fuel cost function to some variables, which linearizes model [M2]. Specifically, the sailing speed on all legs has an influence on the fuel cost function. For a route r, the sailing speed design is solely dependent on the fleet deployment, and is independent of other routes' decisions. Hence, the values of fuel cost function can be obtained with the given fleet deployment through dynamic programming.

We use dynamic programming to obtain an optimal schedule design for route r. Specifically, the dynamic program contains $|I_r|$ stages and the decision at stage i is the determination of sailing time γ_{ri}. The state of stage i, which is the total sailing time allocated to legs $i, i+1, \cdots, |I_r|$, is denoted by s_i. There are two cases for computing s_i. (1) if $i \geq 2$, the set of possible values of s_i is denoted by $S_i =$

$\{\sum_{j=i}^{|I_r|} \lceil T'_{rj} \rceil, \cdots, 7h_r - D_r - \sum_{j=1}^{i-1} \lceil T'_{rj} \rceil\}$, which ensures there is sufficient sailing time allocated to legs $1, \cdots, |I_r|$. (2) If $i = 1$, the possible values of s_1 must be in the set $S_1 := \{7h_r - D_r\}$. Given s_i, the set of possible values of sailing time γ_{ri} is $\{\lceil T'_{ri} \rceil, \cdots, s_i - \sum_{j=i+1}^{|I_r|} \lceil T'_{rj} \rceil\}$. Besides, because the arrival time at the $(i+1)^{st}$ port of call, $\theta_{r,i+1} = \theta_{r1} + 7h_r - (s_i - \gamma_{ri}) - \sum_{j=i+1}^{|I_r|} d_{rj}$, must satisfy the time window, we define the set of possible values of sailing time γ_{ri} as

$$\theta_{ri}(s_i) := \Big\{\gamma_{ri} = \left\lceil T'_{ri} \right\rceil, \cdots, s_i - \sum_{j=i+1}^{|I_r|} \left\lceil T'_{rj} \right\rceil | \\ ((\theta_{r1} + 7h_r - (s_i - \gamma_{ri}) - \sum_{j=i+1}^{|I_r|} d_{rj}) \bmod 7) \in [\theta_{r,i+1}^{min}, \theta_{r,i+1}^{max}]\Big\} \quad \forall i = 1, \cdots, |I_r| - 1. \tag{30}$$

The backward reduction procedure for the problem is described as follows. If the system starts in state s_i at stage i, the corresponding sum of fuel cost on legs $i, \cdots, |I_r|$ is denoted by $u_i(s_i, \gamma_{ri})$. Optimal decisions are made after making the optimal decision of γ_{ri}. The optimal value of γ_{ri} given s_i is denoted by $\gamma_{ri}^*(s_i)$ and $u_i^*(s_i) := u_i(s_i, \gamma_{ri}^*(s_i))$. The recursive relation is

$$u_i^*(s_i) := \min_{\gamma_{ri} \in \Theta_{ri}(s_i)} \Big\{u_i(s_i, \gamma_{ri})\Big\} = \min_{\gamma_{ri} \in \Theta_{ri}(s_i)} \Big\{[\frac{\beta_r^P + \beta_r^\phi}{h_r} f_{ri}^1(\gamma_{ri}) + \frac{\beta_r^S + \beta_r^{SP}}{h_r} f_{ri}^2(\gamma_{ri})] \\ + u_{i+1}^*(s_{i+1})\Big\} \quad \forall s_i \in S_i, i = 1, \cdots, |I_r| - 1 \tag{31}$$

subject to

$$s_{i+1} = s_i - \gamma_{ri} \quad \forall i = 1, \cdots, |I_r| - 1. \tag{32}$$

And the boundary condition is

$$u_{|I_r|}^*(s_{|I_r|}) := \frac{\beta_r^P + \beta_r^\phi}{h_r} f_{r,|I_r|}^1(s_{|I_r|}) + \frac{\beta_r^S + \beta_r^{SP}}{h_r} f_{r,|I_r|}^2(s_{|I_r|}). \tag{33}$$

Because s_1 must be equal to $7h_r - D_r$, the optimal policy that solves $u_1^*(7h_r - D_r)$ provides an optimal solution to the discretized schedule design problem. This method identifies the value of $C_r(\beta_r^{SP}, \beta_r^S, \beta_r^P, \beta_r^\phi)$.

4.3. A proposition for model [M4]

The fleet deployment among routes can be determined in an enumerative manner. In the enumeration process, we do not need to enumerate all possible combinations of ship deployment for each ship route r. The reason is explained in the following proposition.

Proposition 1. *There exists an optimal solution for model [M4], denoted by* ($\beta_r^{SP*}, \beta_r^{S*}, \beta_r^{P*}, \beta_r^{\phi*}, r = 1, \cdots, R$)*, such that each route has only one type of ships (ships with only scrubbers, ships with only shore power, ships with scrubbers and shore power, ships without scrubbers or shore power).*

The proof of the proposition is provided in Appendix 1.

In terms of the fleet deployment, we do not need to enumerate all possible combinations of ship deployment $(\beta_r^{SP}, \beta_r^{S}, \beta_r^{P}, \beta_r^{\phi}) \in \{0, \cdots, h_r\} \times \{0, \cdots, h_r\} \times \{0, \cdots, h_r\} \times \{0, \cdots, h_r\}$. Proposition 1 indicates that a shipping liner should not mix ships with only scrubbers, ships with only shore power, ships with scrubbers and shore power, and ships without scrubbers or shore power on the same liner route. As the fleet deployment of a route is independent of that of the other routes, it can be decomposed for each route. Recalling that we only have four types of ships, based on Proposition 1, we only need to solve model [M4] four times for each route r: all h_r (number of ships deployed on ship route r) ships are ships with scrubbers and shore power, all h_r ships are ships with only scrubbers, all h_r ships are ships with only shore power, and all h_r ships are ships without scrubbers or shore power. An optimal solution for a route r can be obtained by comparing objective values of model [M4] under these four cases.

5. Computational experiments

In order to evaluate the proposed model and assess the efficiency of our algorithm, we perform several computational experiments on a LENOVO P910 workstation (28 cores of CPUs; 2.4 GHz; Memory, 256 GB). The mathematical models and algorithms proposed in this study were implemented in CPLEX 12.5.1 (Visual Studio 2015, $C\#$).

5.1. Experimental setting

We first summarize the setting of our parameter values. The sailing distance data can be acquired from the standard instances *LINER-LIB* (Brouer et al., 2013). The values of c_r^{ϕ},c_r^S,c_r^P, and c_r^{SP} are set to 180,000, 180,829, 180,100, and 180,929 USD/week, respectively (Jiang et al., 2014; Wang et al., 2015; Zhen et al., 2019a). We set the values of m_r^P and m_r^S to 10,000 and 184,298 USD/week (AAPA, 2007; Jiang et al., 2014; Winkel et al., 2016). The average value of h_r depends on the length of cycle time. In 2018, the average values of α_E and α_N are equal to 672.5, and 435.0 USD/ton, respectively (Ship and Bunker, 2019). The average value of c_y^T is 130 USD per TEU (Liu et al., 2014; Zhen et al., 2019b). The minimum and maximum values of the sailing speed ($\underline{e}_{ri}$ and $\overline{e}_{ri}$) are set to eight and 22 knots, respectively, which are also in line with the setting used in related works (Yao et al., 2012; Wang et al., 2015). The average value of c_p^B is set to 1,000 per berth (Zhen et al., 2019a). The value of $\bar{D}$ is two days, which is consistent with related works (Karsten et al., 2017; Zhen et al., 2019a). The average value of v_r of each ship route is set to 17,000 TEU (Meng and Wang, 2012; Zhen et al., 2019b). The value of conversion factors a and b are set to 1.8×10^{-4} and 1.6, respectively (Wang and Meng, 2012). The average value of c_{pq}^D is set to 30 USD per TEU per day (Liu et al., 2014; Zhen et al., 2019b).

5.2. Performance of the algorithm

We apply the three-phase heuristic to solve model [M2]. A large number of numerical experiments over instances with different numbers of routes, physical ports, and ports of call were carried out to validate this algorithm by comparing the values of its solutions with the optimal ones obtained by a method which enumerates the values of the variable γ_{ri} in the model [M2], the optimal ones obtained by a method which solves the model [M3] by the CPLEX directly, and those obtained by the particle swarm optimization (PSO) algorithm which has often been applied to problems solving in the maritime industry (De et al., 2016, 2017; Jeong et al., 2018; Zheng et al., 2019; Le Carrer et al., 2020). The algorithms' performance is measured in terms of CPU time, and in terms of the gap between the results obtained by these four methods.

Table 2 and Table 3 list the comparison between the enumeration method, the CPLEX method, the PSO algorithm, and the proposed three-phase method. (1) The enumeration method is to replace the complex fuel function with a parameter by enumerating the function's variables γ_{ri}. After this substitution, the model can be solved by the CPLEX directly. The result can be regarded as an optimal solution for the model [M2]. (2) The model [M3] can be solved by the CPLEX directly to obtain optimal results. (3) By applying the fuel cost function transformation in three-phase heuristic, model [M2] can be tractable by the PSO algorithm. An introduction to the PSO algorithm is provided in Appendix 4. (4) In our proposed three-phase solution method, the loss of optimality is mainly caused by the "approximate division" in the second phase. The third phase "solution improvement" cannot guarantee that the solution could be improved to optimality. Therefore, the comparative results in Table 2 and Table 3 should reflect the quality loss of the second and third phases in our proposed solution method.

In Tables 2 and 3, "Obj" represents the objective function values of the model, which are the total costs of the solutions generated by the enumeration method, the CPLEX method, the three-phase heuristic and the PSO algorithm. "Time" represents the CPU running time, "Gap_{obj}^{T}" records the gap between objective function values solved by the CPLEX directly and those of the three-phase heuristic ($Gap_{obj}^{T} = \frac{|Obj_{\text{three-phase}} - Obj_{\text{CPLEX}}|}{Obj_{\text{CPLEX}}} \times 100$), and "$Gap_{obj}^{P}$" records the gap between objective function values solved by the three-phase heuristic and those of the PSO algorithm ($Gap_{obj}^{P} = \frac{|Obj_{\text{PSO}} - Obj_{\text{three-phase}}|}{Obj_{\text{three-phase}}} \times 100$). From Table 2, we see that although the enumeration method can find the optimal solution, the solution time of the enumeration method is the longest. Besides, the objective values obtained by the three-phase heuristic are equal to the optimal results solved by the CPLEX directly, but our heuristic is always much faster. From Table 3, the objective values obtained by the three-phase heuristic are also closer to the exact solutions obtained by the enumeration method than the objective values obtained by the PSO algorithm. The computational time by the PSO algorithm is longer than that of the three-phase heuristic. These results validate the efficiency of the three-phase heuristic.

5.3. Sensitivity analysis and managerial insights

In this study, parameters such as fuel oil price, scrubbers and shore power installation cost, and weekly operating cost of ships are set as constants. In practice, however, these factors fluctuate considerably. With the development of the manufac-

Table 2: Comparison between the enumeration method, the CPLEX method and the three-phase heuristic

Case ID	Enumeration method		CPLEX method		Three-phase heuristic			
	Obj^E	$Time^E$ (s)	Obj^C	$Time^C$ (s)	Obj^T	$Time^T$ (s)	Gap^T_{obj}(%)	$\frac{Time^T}{Time^C}$
Case 1 (2,6,6)	22,318,673	15	22,318,673	3	22,318,673	2	0	0.67
Case 2 (2,5,8)	–	$\geq$ 3,600	60,546,407	8	60,546,407	4	0	0.50
Case 3 (2,6,11)	–	$\geq$ 3,600	91,938,052	21	91,938,052	9	0	0.43
Case 4 (3,8,11)	–	$\geq$ 3,600	68,870,403	20	68,870,403	6	0	0.30
Case 5 (3,9,12)	–	$\geq$ 3,600	68,524,396	15	68,524,396	10	0	0.67
Case 6 (3,8,14)	–	$\geq$ 3,600	100,558,167	33	100,558,167	14	0	0.42
Case 7 (4,9,17)	–	$\geq$ 3,600	114,899,740	40	114,899,740	17	0	0.40

* Notes: In "Case ID", the three values within parentheses denote the number of ship routes, physical ports, and ports of call, respectively. The en-dash means that we did not find any solution within one hour.

Table 3: Comparison between the three-phase heuristic and the PSO heuristic

Case ID	Three-phase heuristic		PSO heuristic			
	Obj^T	$Time^T$ (s)	Obj^P	$Time^P$ (s)	Gap^P_{obj}(%)	$\frac{Time^T}{Time^P}$
Case 1 (2,6,6)	22,318,673	2	22,318,673	193	0.00	0.01
Case 2 (2,5,8)	60,546,407	4	60,546,407	417	0.00	0.01
Case 3 (2,6,11)	91,938,052	9	92,010,548	879	0.08	0.01
Case 4 (3,8,11)	68,870,403	6	68,919,935	503	0.07	0.01
Case 5 (3,9,12)	68,524,396	10	68,629,959	1,190	0.15	0.01
Case 6 (3,8,14)	100,558,167	14	100,680,196	2,611	0.12	0.01
Case 7 (4,9,17)	114,899,740	17	115,028,266	3,531	0.11	$<$ 0.01

* Notes: In "Case ID", the three values within parentheses denote the number of ship routes, physical ports, and ports of call, respectively.

turing industry, technologies related to both scrubbers and shore power will mature, which will surely result in a cost decrease in the production of scrubbers and shore power, and will have an influence on fleet deployment. In this section, we show how fleet deployment decisions would respond when facing with these changes.

There are two types of fuel used for ships. In ECAs, ships that are not equipped with scrubbers need use the MGO, rather than the HFO, so as to reduce local SO_X emissions. However, the MGO is much more expensive than the HFO. We found that from 2016 to 2018, the lowest and highest prices of global average bunker price of the MGO fuel oil were 387.5 and 786.0 USD/ton, respectively, while the lowest and highest prices of HFO were 166.5 and 514.5 USD/ton, respectively (Ship and Bunker, 2019).

We first discuss the impact of an increase in fuel oil price on fleet deployment decisions where the HFO fuel oil price α_N ranges from 150 to 500 USD/ton, and the MGO fuel oil price α_E ranges from 350 to 800 USD/ton. The results for the deployment of four types of ships are reported in Table 4 (columns 4 to 7). We consider an example with four routes and 17 ports of call. β^S, β^P, β^{SP} and β^ϕ represent the numbers of deployed ships with only scrubbers, with only shore power, with scrubbers and shore power, without scrubbers or shore power, respectively. The last two columns on the right are the ratio of the number of ships with scrubbers to the total number of ships, and the ratio of the number of ships with shore power to the total number of ships. It is obvious that the increase in fuel oil price has little effect on the decision whether ships are equipped with shore power or not, but has a significant impact on the number of ships with scrubbers. To be specific, as the price difference between HFO and MGO increases, the demand for scrubbers also increases. As shown in Figure 2, we draw three lines for the price of MGO (350, 500, 800 USD/ton), plotted by the ratio of the HFO price with MGO price on the horizontal axis and the ratio of the number of ships with scrubbers to the total number of ships on the vertical axis. We note that as the price of MGO increases, the demand for scrubbers is more sensitive to the price difference between HFO and MGO. Besides, when the ratio of the HFO price to the MGO price reaches a certain point, the ratio of the number of ships with scrubbers to the total number of ships remains unchanged, which means that the fluctuations in global oil prices do not always influence the decision to equip ships with scrubbers or not.

The trend observed in Table 4 shows that, in general, the number of ships with scrubbers increases with an increase in fuel price. This result is as expected because as the fuel switching cost increases in ECAs, it becomes more profitable to install scrubbers for ships to avoid using MGO. However, note that the ratio of the number

Table 4: Impact of fuel oil price on fleet deployment

Case ID	α_N	α_E	β^S	β^P	β^{SP}	β^ϕ	$\frac{\beta^S+\beta^{SP}}{\sum_{r=1}^R h_r}$	$\frac{\beta^P+\beta^{SP}}{\sum_{r=1}^R h_r}$
Case 1	150	350	6	0	0	5	0.55	0.00
Case 2	200	350	6	0	0	5	0.55	0.00
Case 3	250	350	0	0	0	11	0.00	0.00
Case 4	300	350	0	0	0	11	0.00	0.00
Case 5	200	500	6	0	0	5	0.55	0.00
Case 6	300	500	6	0	0	5	0.55	0.00
Case 7	400	500	2	0	0	9	0.18	0.00
Case 8	450	500	0	0	0	11	0.00	0.00
Case 9	200	800	11	0	0	0	1.00	0.00
Case 10	300	800	11	0	0	0	1.00	0.00
Case 11	400	800	11	0	0	0	1.00	0.00
Case 12	500	800	8	0	0	3	0.73	0.00

of ships with scrubbers to the total number of ships when the prices of HFO and MGO are 435.0 and 672.5 USD/ton (current fuel oil prices), respectively, is 0.55. This conflicts with the current situation, not many ships have scrubbers because it costs three to five million USD to install a scrubber (UNCTAD, 2015). However, according to related studies (Jiang et al., 2014), the life span of scrubbers is 12 years. It is then economically preferable ($\frac{3{,}000{,}000\times0.02\times1.02^{12\times52}}{1.02^{12\times52}-1}\approx 60,000$ USD/week) for shipping companies to install a scrubber for ships in consideration of increasingly expensive fuel switching cost, and higher weekly operating cost of a normal ship (180,000 USD/week (Wang and Meng, 2015; Wang et al., 2015)). Clearly, in order to curb SO_X emissions within a larger number of ECAs in the future, equipping ships with scrubbers is the first choice for shipping companies. On the other hand, the effect of an increase in fuel price on the number of ships with scrubbers seems bigger than that of ships with shore power (two rightmost columns). This result is also as expected because fuel consumed by ships on a voyage is much more than fuel consumed by ships during dwell at ports.

Next we analyse the impacts of weekly operating cost and initial installation cost

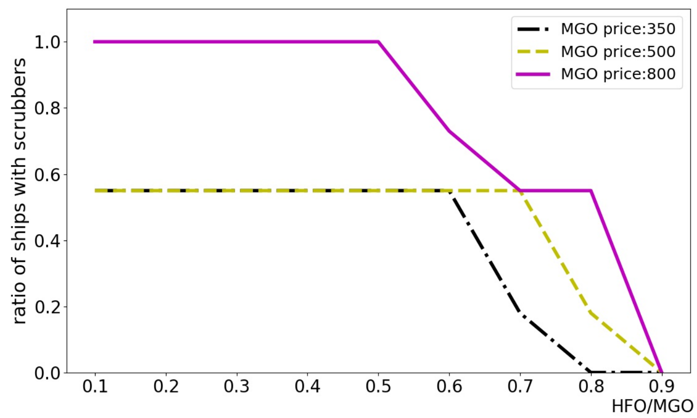

Figure 2: Impact of fuel oil price ratio on fleet deployment

of scrubbers. The costs related to scrubbers influence the fleet deployment. Taking an example of four ports and 17 ports of call, Table 5 demonstrates the effects of the weekly operating cost of scrubbers (c_r^S) and of the initial installation cost of scrubbers (m_r^S). The value of c_r^S is set to 200,000, 190,000, and 180,000 USD/week, respectively, m_r^S is set to 184,298, 154,298, and 84,298 USD/week, respectively. As shown in Table 5, we find that more ships with scrubbers are needed when the initial installation cost decreases, which implies that many shipping companies are likely to buy cheaper and cheaper scrubbers, and install scrubbers on ships. Besides, the number of ships with scrubbers does not change as the weekly operating cost decreases. This implies that the initial installation cost has a more significant influence on the adoption of scrubbers than the weekly operating cost. As the scrubber technology will mature, the initial installation cost will decrease and more shipping companies will prefer to retrofit ships by installing scrubbers rather than switching to expensive MGO in ECAs.

To study the impact of the initial installing shore power cost, we test an instance that consists of four routes and 17 ports of call. In Table 6, m_r^P reports the initial shore power installation cost and is set to 10,000, 6,000, 4,000 and 1,000 USD/week, respectively. The shore power is the conversion between sockets and electrical equipment while scrubbers need to be replaced with an alkaline solution. Hence, the weekly

Table 5: Impacts of weekly operating cost and initial installation cost of scrubbers on fleet deployment

Case ID	c_r^S	m_r^S	β^S	β^P	β^{SP}	β^ϕ	$\frac{\beta^S+\beta^{SP}}{\sum_{r=1}^R h_r}$
Case 1	200,000	184,298	0	0	6	5	0.55
Case 2	190,000	184,298	0	0	6	5	0.55
Case 3	180,000	184,298	6	0	0	5	0.55
Case 4	200,000	154,298	0	0	6	5	0.55
Case 5	190,000	154,298	0	0	6	5	0.55
Case 6	180,000	154,298	6	0	0	5	0.55
Case 7	200,000	84,298	0	0	11	0	1.00
Case 8	190,000	84,298	0	0	11	0	1.00
Case 9	180,000	84,298	11	0	0	0	1.00

operating cost of shore power is rather low, and this study only considers the impact of the initial installing of shore power cost on fleet deployment. More and more ships with shore power are needed when the initial installation cost of shore power decreases, which will occur in the future because of the development of mature technologies. Apart from the above-mentioned conclusions, we also explore the impact of extra cost for a ship with shore power mooring at a berth without shore power on fleet deployment. From Table 7, we see that the increase in extra cost for a ship with shore power mooring at a berth without shore power always leads to an increasing number of ships with shore power. In this study, c_p^B denotes the extra cost for a ship with shore power mooring at a berth without shore power, which also results in a saving if a ship with shore power mooring at a berth is equipped with shore power. In this case, the larger is the cost saving, the more ships should be equipped with shore power.

Finally, we study the impact of the ECA boundary on the fleet deployment. The ECA boundary can directly influence the fuel cost inside and outside the ECAs, the strategy on changing fuels or installing new equipment. In Table 8, L denotes the extended distance of ECAs toward out seas. The value of L is set as 1, 5, 12, 30, 50, 100, and 150 nautical miles. Table 8 shows that as the extended distance increases,

Table 6: Impact of initial installation cost of shore power on fleet deployment

Case ID	m_r^P	β^S	β^P	β^{SP}	β^{ϕ}	$\frac{\beta^P+\beta^{SP}}{\sum_{r=1}^R h_r}$
Case 1	10,000	6	0	0	5	0.00
Case 2	6,000	6	0	0	5	0.00
Case 3	4,000	6	0	0	5	0.00
Case 4	1,000	0	5	6	0	1.00

Table 7: Impact of extra cost for a ship with shore power mooring at a berth without shore power on fleet deployment

Case ID	c_p^B	β^S	β^P	β^{SP}	β^{ϕ}	$\frac{\beta^P+\beta^{SP}}{\sum_{r=1}^R h_r}$
Case 1	1,000	6	0	0	5	0.00
Case 2	3,000	6	0	0	5	0.00
Case 3	5,000	6	0	0	5	0.00
Case 4	8,000	0	5	6	0	1.00

the number of ships with scrubbers also increases. This result is reasonable because a longer extended distance translates into a longer sailing distance within the ECAs, which further implies that the fuel switching cost becomes higher. In this case, the shipping companies are willing to initially install scrubbers instead of bearing more expensive fuel switching costs. Moreover, the ECA boundary has a greater effect on the decision to install scrubbers or not than that on the decision to install shore power or not, because the ratio of the number of ships with shore power to the total number of ships (the rightmost column) remains unchanged as the extended distance increases, while the ratio related to the scrubbers grows (the column $\frac{\beta^S+\beta^{SP}}{\sum_{r=1}^R h_r}$).

Table 8: Impact of ECA boundary on fleet deployment

Case ID	L	β^S	β^P	β^{SP}	β^ϕ	$\frac{\beta^S+\beta^{SP}}{\sum_{r=1}^R h_r}$	$\frac{\beta^P+\beta^{SP}}{\sum_{r=1}^R h_r}$
Case 1	1	6	0	0	5	0.55	0.00
Case 2	5	6	0	0	5	0.55	0.00
Case 3	12	6	0	0	5	0.55	0.00
Case 4	30	8	0	0	3	0.73	0.00
Case 5	50	11	0	0	0	1.00	0.00
Case 6	100	11	0	0	0	1.00	0.00

6. Conclusions

We have investigated an integrated optimization problem, which includes deploying ships equipped with different green technologies among routes, timetables, sailing speed on all legs, and cargo allocation among routes for each OD pair, in the context of ECAs. We considered some frequently ignored realistic factors, such as transshipment activities, berth limitations, and transit time requirements. It is obvious that these factors complicate this problem but make our proposed methodology fit the realistic needs of the shipping industry against the background of stricter ECA regulations that are being implemented around the world. Owing to the complexity of the proposed model, we used some techniques to linearize it and we developed a novel three-phase heuristic to solve instances efficiently. This study makes three main scientific contributions:

(1) It integrates several interconnected decisions in the context of ECAs: deployment decisions of different types of ships with respect to their equipped green technologies, timetables, the determination of sailing speed on all legs, and the allocation of cargo among routes for each OD pair. Several realistic factors, such as transshipment activities, berth limitations, and transit time requirements, were also considered. Moreover, green technology adoption was embedded in the problem. No previous studies have considered these factors simultaneously and have integrated them within a solution methodology.

(2) To handle the proposed model, some linearization techniques were applied,

and a novel three-phase heuristic was designed to solve the problem. We found that our algorithm is computationally efficient for the proposed model, on the basis of extensive numerical experiments. Our results indicate that the algorithm we have developed yields optimal solutions on all instances, and can solve realistic instances with four routes and 17 ports of call within 17 seconds.

(3) After conducting quantitative computational experiments, we derived some managerial implications on fleet deployment, service schedule design, and cargo allocation for shipping companies under ECA regulations. For instance, the best fleet deployment plan is that in which each route uses only one type of ship with respect to their equipped green technologies.

Acknowledgments

This work was supported by the National Natural Science Foundation of China [grant number 71831008, 71671107], by the Research Grants Council of the Hong Kong Special Administrative Region, China [project number 15201718], by the Canadian Network for Research and Innovation in Machining Technology, and by the Natural Sciences and Engineering Research Council of Canada [grant number 2015-06189]. Thanks are due to the referees for their valuable comments.

References

AAPA, 2007. Use of shore-side power for ocean-going vessels white paper (accessed on 27 February 2019).
URL `http://wpci.iaphworldports.org/data/docs/onshore-power-supply/library/1264151248_2007aapauseofshore-sidepowerforocean-goingvessels.pdf`.

Acciaro, M., 2014. Real option analysis for environmental compliance: LNG and emission control areas. Transportation Research Part D: Transport and Environment 28, 41–50.

Agarwal, R., Ergun, Ö., 2008. Ship scheduling and network design for cargo routing in liner shipping. Transportation Science 42 (2), 175–196.

Armellini, A., Daniotti, S., Pinamonti, P., Reini, M., 2018. Evaluation of gas turbines as alternative energy production systems for a large cruise ship to meet new maritime regulations. Applied Energy 211, 306–317.

Atari, S., Prause, G., 2017. Risk assessment of emission abatement technologies for clean shipping. In: International Conference on Reliability and Statistics in Transportation and Communication. Riga, pp. 93–101.

Bakkehaug, R., Rakke, J. G., Fagerholt, K., Laporte, G., 2016. An adaptive large neighborhood search heuristic for fleet deployment problems with voyage separation requirements. Transportation Research Part C: Emerging Technologies 70, 129–141.

Bektaş, T., Ehmke, J. F., Psaraftis, H. N., Puchinger, J., 2019. The role of operational research in green freight transportation. European Journal of Operational Research 274, 807–823.

Bell, M. G. H., Liu, X., Angeloudis, P., Fonzone, A., Hosseinloo, S. H., 2011. A frequency-based maritime container assignment model. Transportation Research Part B: Methodological 45 (8), 1152–1161.

Bell, M. G. H., Liu, X., Rioult, J., Angeloudis, P., 2013. A cost-based maritime container assignment model. Transportation Research Part B: Methodological 58, 58–70.

Brouer, B. D., Alvarez, J. F., Plum, C. E., Pisinger, D., Sigurd, M. M., 2013. A base integer programming model and benchmark suite for liner-shipping network design. Transportation Science 48 (2), 281–312.

Brouer, B. D., Karsten, C. V., Pisinger, D., 2017. Optimization in liner shipping. 4OR 15 (1), 1–35.

Brynolf, S., Magnusson, M., Fridell, E., Andersson, K., 2014. Compliance possibilities for the future ECA regulations through the use of abatement technologies or change of fuels. Transportation Research Part D: Transport and Environment 28, 6–18.

Cariou, P., 2011. Is slow steaming a sustainable means of reducing CO_2 emissions from container shipping? Transportation Research Part D: Transport and Environment 16 (3), 260–264.

Chen, W., Panahi, M., Tsangaratos, P., Shahabi, H., Ilia, I., Panahi, S., Li, S., Jaafari, A., Ahmad, B. B., 2019. Applying population-based evolutionary algorithms and a neuro-fuzzy system for modeling landslide susceptibility. Catena 172, 212–231.

Christiansen, M., Fagerholt, K., Nygreen, B., Ronen, D., 2013. Ship routing and scheduling in the new millennium. European Journal of Operational Research 228 (3), 467–483.

Christiansen, M., Fagerholt, K., Ronen, D., 2004. Ship routing and scheduling: Status and perspectives. Transportation Science 38 (1), 1–18.

Clerc, M., 2010. Particle Swarm Optimization. Wiley, Hoboken, New Jersey.

Corbett, J. J., Wang, H., Winebrake, J. J., 2009. The effectiveness and costs of speed reductions on emissions from international shipping. Transportation Research Part D: Transport and Environment 14 (8), 593–598.

De, A., Kumar, S. K., Gunasekaran, A., Tiwari, M. K., 2017. Sustainable maritime inventory routing problem with time window constraints. Engineering Applications of Artificial Intelligence 61, 77–95.

De, A., Mamanduru, V. K. R., Gunasekaran, A., Subramanian, N., Tiwari, M. K., 2016. Composite particle algorithm for sustainable integrated dynamic ship routing and scheduling optimization. Computers & Industrial Engineering 96, 201–215.

Deng, W., Zhao, H., Yang, X., Xiong, J., Sun, M., Li, B., 2017. Study on an improved adaptive pso algorithm for solving multi-objective gate assignment. Applied Soft Computing 59, 288–302.

Du, G., Sun, C., Weng, J., 2016. Liner shipping fleet deployment with sustainable collaborative transportation. Sustainability 8 (2), 165.

Eberhart, R., Kennedy, J., 1995. A new optimizer using particle swarm theory. In: MHS'95. Proceedings of the Sixth International Symposium on Micro Machine and Human Science. IEEE 39–43.

Fagerholt, K., Gausel, N. T., Rakke, J. G., Psaraftis, H. N., 2015. Maritime routing and speed optimization with emission control areas. Transportation Research Part C: Emerging Technologies 52, 57–73.

Fagerholt, K., Johnsen, T. A., Lindstad, H., 2009. Fleet deployment in liner shipping: a case study. Maritime Policy & Management 36 (5), 397–409.

Fagerholt, K., Psaraftis, H. N., 2015. On two speed optimization problems for ships that sail in and out of emission control areas. Transportation Research Part D: Transport and Environment 39, 56–64.

Fransoo, J. C., Lee, C.-Y., 2013. The critical role of ocean container transport in global supply chain performance. Production and Operations Management 22 (2), 253–268.

IMO, 2016. International maritime of organization website (accessed on 27 February 2019).
URL http://www.imo.org/en/OurWork/Environment/PollutionPrevention/AirPollution/Pages/Air-Pollution.aspx.

Innes, A., Monios, J., 2018. Identifying the unique challenges of installing cold ironing at small and medium ports–the case of aberdeen. Transportation Research Part D: Transport and Environment 62, 298–313.

IOoSM, 2018. Information office of shanghai municipality website (accessed on 25 August 2019).
URL http://www.shio.gov.cn/sh/xwb/n782/n783/u1ai17513.html.

Jeong, Y., Saha, S., Chatterjee, D., Moon, I., 2018. Direct shipping service routes with an empty container management strategy. Transportation Research Part E: Logistics and Transportation Review 118, 123–142.

Jiang, L., Kronbak, J., Christensen, L. P., 2014. The costs and benefits of sulphur reduction measures: Sulphur scrubbers versus marine gas oil. Transportation Research Part D: Transport and Environment 28, 19–27.

Karsten, C. V., Brouer, B. D., Desaulniers, G., Pisinger, D., 2017. Time constrained liner shipping network design. Transportation Research Part E: Logistics and Transportation Review 105, 152–162.

Khersonsky, Y., Islam, M., Peterson, K., 2007. Challenges of connecting shipboard marine systems to medium voltage shoreside electrical power. IEEE Transactions on Industry Applications 43 (3), 838–844.

Kontovas, C., Psaraftis, H. N., 2011. Reduction of emissions along the maritime intermodal container chain: operational models and policies. Maritime Policy & Management 38 (4), 451–469.

Lai, K.-H., Lun, V. Y., Wong, C. W., Cheng, T., 2011. Green shipping practices in the shipping industry: Conceptualization, adoption, and implications. Resources, Conservation and Recycling 55 (6), 631–638.

Le Carrer, N., Ferson, S., Green, P. L., 2020. Optimising cargo loading and ship scheduling in tidal areas. European Journal of Operational Research 280 (3), 1082–1094.

Lee, C.-Y., Song, D.-P., 2017. Ocean container transport in global supply chains: Overview and research opportunities. Transportation Research Part B: Methodological 95, 442–474.

Lin, D.-Y., Chang, Y.-T., 2018. Ship routing and freight assignment problem for liner shipping: Application to the northern sea route planning problem. Transportation Research Part E: Logistics and Transportation Review 110, 47–70.

Liu, Z., Meng, Q., Wang, S., Sun, Z., 2014. Global intermodal liner shipping network design. Transportation Research Part E: Logistics and Transportation Review 61, 28–39.

Meng, Q., Wang, S., 2012. Liner ship fleet deployment with week-dependent container shipment demand. European Journal of Operational Research 222 (2), 241–252.

Meng, Q., Wang, S., Andersson, H., Thun, K., 2013. Containership routing and scheduling in liner shipping: overview and future research directions. Transportation Science 48 (2), 265–280.

Meng, Q., Wang, T., Wang, S., 2012. Short-term liner ship fleet planning with container transshipment and uncertain container shipment demand. European Journal of Operational Research 223 (1), 96–105.

Nasir, M., Das, S., Maity, D., Sengupta, S., Halder, U., Suganthan, P. N., 2012. A dynamic neighborhood learning based particle swarm optimizer for global numerical optimization. Information Sciences 209, 16–36.

Ölçer, A., Ballini, F., 2015. The development of a decision making framework for evaluating the trade-off solutions of cleaner seaborne transportation. Transportation Research Part D: Transport and Environment 37, 150–170.

Patricksson, Ø. S., Fagerholt, K., Rakke, J. G., 2015. The fleet renewal problem with regional emission limitations: Case study from roll-on/roll-off shipping. Transportation Research Part C: Emerging Technologies 56, 346–358.

Plakantonaki, C., 2017. Scrubber realities: The ship operator perspective (accessed on 6 September 2019).
URL `https://safety4sea.com/cm-scrubber-realities-the-ship-operator/-perspective/`.

Psaraftis, H. N., 2016. Green Transportation Logistics. Springer International Publishing, Heidelberg.

Reinhardt, L. B., Plum, C. E., Pisinger, D., Sigurd, M. M., Vial, G. T., 2016. The liner shipping berth scheduling problem with transit times. Transportation Research Part E: Logistics and Transportation Review 86, 116–128.

Ren, J., Lützen, M., 2015. Fuzzy multi-criteria decision-making method for technology selection for emissions reduction from shipping under uncertainties. Transportation Research Part D: Transport and Environment 40, 43–60.

Ronen, D., 1993. Ship scheduling: The last decade. European Journal of Operational Research 71 (3), 325–333.

Sciberras, E. A., Zahawi, B., Atkinson, D. J., 2015. Electrical characteristics of cold ironing energy supply for berthed ships. Transportation Research Part D: Transport and Environment 39, 31–43.

Shi, Y., 2001. Particle swarm optimization: developments, applications and resources. In: Proceedings of the 2001 congress on evolutionary computation (IEEE Cat. No. 01TH8546). Vol. 1. IEEE, pp. 81–86.

Shi, Y., Eberhart, R., 1998. A modified particle swarm optimizer. In: 1998 IEEE international conference on evolutionary computation proceedings. IEEE world congress on computational intelligence (Cat. No. 98TH8360). IEEE, pp. 69–73.

Ship and Bunker, 2019. World bunker prices (accessed on 27 February 2019). URL `https://shipandbunker.com/prices/av/global/av-g20-global-20-ports-average`.

Soleimani, H., Kannan, G., 2015. A hybrid particle swarm optimization and genetic algorithm for closed-loop supply chain network design in large-scale networks. Applied Mathematical Modelling 39 (14), 3990–4012.

Song, D.-P., Dong, J.-X., 2013. Long-haul liner service route design with ship deployment and empty container repositioning. Transportation Research Part B: Methodological 55, 188–211.

UNCTAD, 2015. Review of Maritime Transportation 2015 (accessed on 27 February 2019). URL `http://unctad.org/en/PublicationsLibrary/rmt2015_en.pdf`.

Üster, H., Hwang, S. O., 2016. Closed-loop supply chain network design under demand and return uncertainty. Transportation Science 51 (4), 1063–1085.

Wang, S., Meng, Q., 2012. Sailing speed optimization for container ships in a liner shipping network. Transportation Research Part E: Logistics and Transportation Review 48 (3), 701–714.

Wang, S., Meng, Q., 2015. Robust bunker management for liner shipping networks. European Journal of Operational Research 243 (3), 789–797.

Wang, S., Zhuge, D., Zhen, L., Lee, C.-Y., 2019. Liner shipping service planning under sulphur emission regulations,Working paper.

Wang, Y., Meng, Q., Du, Y., 2015. Liner container seasonal shipping revenue management. Transportation Research Part B: Methodological 82, 141–161.

Wen, M., Pacino, D., Kontovas, C., Psaraftis, H. N., 2017. A multiple ship routing and speed optimization problem under time, cost and environmental objectives. Transportation Research Part D: Transport and Environment 52, 303–321.

Winkel, R., Weddige, U., Johnsen, D., Hoen, V., Papaefthimiou, S., 2016. Shore side electricity in Europe: Potential and environmental benefits. Energy Policy 88, 584–593.

Xia, J., Li, K. X., Ma, H., Xu, Z., 2015. Joint planning of fleet deployment, speed optimization, and cargo allocation for liner shipping. Transportation Science 49 (4), 922–938.

Yang, Z. L., Zhang, D., Caglayan, O., Jenkinson, I., Bonsall, S., Wang, J., Huang, M., Yan, X., 2012. Selection of techniques for reducing shipping NO_X and SO_X emissions. Transportation Research Part D: Transport and Environment 17 (6), 478–486.

Yao, Z., Ng, S. H., Lee, L. H., 2012. A study on bunker fuel management for the shipping liner services. Computers & Operations Research 39 (5), 1160–1172.

Zhang, Z.-H., Berenguer, G., Shen, Z.-J., 2014. A capacitated facility location model with bidirectional flows. Transportation Science 49 (1), 114–129.

Zhen, L., Hu, Y., Wang, S., Laporte, G., Wu, Y., 2019a. Fleet deployment and demand fulfillment for container shipping liners. Transportation Research Part B: Methodological 120, 15–32.

Zhen, L., Li, M., Hu, Z., Lv, W., Zhao, X., 2018. The effects of emission control area regulations on cruise shipping. Transportation Research Part D: Transport and Environment 62, 47–63.

Zhen, L., Wang, S., Laporte, G., Hu, Y., 2019b. Integrated planning of ship deployment, service schedule and container routing. Computers & Operations Research 104, 304–318.

Zhen, L., Zhuge, D., Murong, L., Yan, R., Wang, S., 2019c. Operation management of green ports and shipping networks: overview and research opportunities. Frontiers of Engineering Management 6 (2), 152–162.

Zheng, J., Zhang, H., Yin, L., Liang, Y., Wang, B., Li, Z., Song, X., Zhang, Y., 2019. A voyage with minimal fuel consumption for cruise ships. Journal of Cleaner Production 215, 144–153.

Zis, T., Psaraftis, H. N., 2017. The implications of the new sulphur limits on the European Ro-Ro sector. Transportation Research Part D: Transport and Environment 52, 185–201.

Appendix 1: Proof of Proposition 1

Proof. Suppose there exists an optimal solution in which at least one route has at least two types of ships. For the ease of writing, we consider two types of ships (ships with scrubbers, ships without scrubbers or shore power) as an example. We sort the routes in the following way and denote the sorted routes as $1, \cdots, |R|$:

$$
\begin{aligned}
& [c_1^{\phi} + \frac{f_{1,i}^1(\gamma_{1,i}^*)}{h_1} + \sum_{i \in I_1} \sum_{n=0}^{h_1} \frac{c_p^B \alpha_{1in\hat{b}} n}{h_1}] - [c_1^S + \frac{f_{1,i}^2(\gamma_{1,i}^*)}{h_1} + \sum_{i \in I_1} \sum_{n=0}^{h_1} \frac{c_p^B \alpha_{1in\hat{b}} n}{h_1}] \\
\geq \ & [c_2^{\phi} + \frac{f_{2,i}^1(\gamma_{2,i}^*)}{h_2} + \sum_{i \in I_2} \sum_{n=0}^{h_2} \frac{c_p^B \alpha_{2in\hat{b}} n}{h_2}] - [c_2^S + \frac{f_{2,i}^2(\gamma_{2,i}^*)}{h_2} + \sum_{i \in I_2} \sum_{n=0}^{h_2} \frac{c_p^B \alpha_{2in\hat{b}} n}{h_2}] \\
\geq \ & \cdots \\
\geq \ & [c_R^{\phi} + \frac{f_{R,i}^1(\gamma_{R,i}^*)}{h_R} + \sum_{i \in I_R} \sum_{n=0}^{h_R} \frac{c_p^B \alpha_{Rin\hat{b}} n}{h_R}] - [c_R^S + \frac{f_{R,i}^S(\gamma_{R,i}^*)}{h_R} + \sum_{i \in I_R} \sum_{n=0}^{h_R} \frac{c_p^B \alpha_{Rin\hat{b}} n}{h_R}].
\end{aligned}
\tag{34}
$$

That is, the cost reduction obtained by replacing a ship without scrubbers on route 1 with a ship with scrubbers is the largest, the cost reduction of such a replacement for route 2 is the second largest, etc. Then, we can derive a new solution: the total number of ships deployed on each route is unchanged, we replace ships without scrubbers by ships with scrubbers if the difference value of the above formula of those routes which have two types of ships is positive, and we replace ships with scrubbers by ships without scrubbers if the difference value is negative. In this case, each route only has one type of ship. This new solution is at least as good as the optimal one, and hence is also optimal. Besides, in this new solution all routes contain only one type of ship. □

Appendix 2: Model reformulation 1

Proof. We have developed some techniques to linearize the nonlinear functions of [M1] in the following subsections. The specific transformation process of model [M2] is summarized below.

1.1. Linearization process of the function of extra cost for berths without shore power in objective function (4)

In the objective function, the extra cost for berths without shore power $\sum_{r\in R}\sum_{i\in I_r} \frac{\beta_r^{SP}+\beta_r^P}{h_r} c_p^B \lambda_{ri\hat{b}}$ contains the product of variable $(\beta_r^{SP}+\beta_r^P)$ with the variable $\lambda_{ri\hat{b}}$. To linearize this form, some newly defined variables and constraints are added as follows.

Newly defined big-M's:

M_r	Big-M for linearization.

Newly defined variables:

$\alpha_{rin\hat{b}}$	set to one if and only if the number of ships with shore power and ships with both scrubbers and shore power at the berth $\hat{b}$ in the i^{th} port of call on ship route r is n, and zero otherwise.

In addition, some additional constraints need to be defined so that the newly variable $\alpha_{rin\hat{b}}$ can replace the function of $(\beta_r^{SP}+\beta_r^P)\lambda_{ri\hat{b}}$.

Newly defined constraints:

$$\alpha_{rin\hat{b}} \;\leq\; \lambda_{ri\hat{b}} \quad \forall r\in R, i\in I_r, n\in\{1,\cdots,h_r\} \tag{35}$$

$$\sum_{n=0}^{h_r}\alpha_{rin\hat{b}} = 1 \quad \forall r\in R, i\in I_r \tag{36}$$

$$\sum_{n=0}^{h_r}\alpha_{rin\hat{b}}n \;\leq\; \beta_r^P+\beta_r^{SP} \quad \forall r\in R, i\in I_r \tag{37}$$

$$\sum_{n=0}^{h_r}\alpha_{rin\hat{b}}n \;\geq\; \beta_r^P+\beta_r^{SP}+(\lambda_{ri\hat{b}}-1)M_r \quad \forall r\in R, i\in I_r \tag{38}$$

$$\alpha_{rin\hat{b}}\in\{0,1\} \quad \forall r\in R, i\in I_r, n\in\{0,\cdots,h_r\}. \tag{39}$$

The big-M in Constraints (38) can be set as $M_r = h_r$ because $\beta_r^P + \beta_r^{SP} \le h_r$. Then the nonlinear form $\sum_{r\in R}\sum_{i\in I_r} \frac{\beta_r^{SP}+\beta_r^P}{h_r} c_p^B \lambda_{ri\hat{b}}$ in the objective (4) is replaced with the linearized form $\sum_{r\in R}\sum_{i\in I_r}\sum_{n=0}^{h_r} \frac{c_p^B \alpha_{rin\hat{b}} n}{h_r}$.

1.2. Linearization process of the function of service level related penalty in objective function (4)

The penalty cost in the objective "$\sum_{p\in P}\sum_{q\in P}\sum_{y\in Y_{pq}} \pi_y c_{pq}^D (\tau_y - T_{pq})^{+}$" contains the product of variable π_y with variable $(\tau_y - T_{pq})^+$. Moreover, the form "$(\cdot)^+$" is also nonlinear. To linearize the penalty cost, some more variables and constraints are added as follows.

Newly defined index and sets:

t	index of the number of days, which represents the delay of an OD delivery.
T_{pqy}^{DEL}	set of possible values of t for the transportation plan y of OD $\langle p, q\rangle$; $T_{pqy}^{DEL} = \{(\underline{\tau}_y - T_{pq})^+, (\underline{\tau}_y - T_{pq})^+ + 1, \cdots, (\overline{\tau}_y - T_{pq})^+\}$. Here x^+ :=max$\{x, 0\}$ and for τ_y, its lower bound $\underline{\tau}_y$ and upper bound $\overline{\tau}_y$ are calculated by Eq. (40)–(41), respectively:

$$\underline{\tau}_y = \sum_{r\in R}\sum_{i\in I_r} k_{yri}(\left\lceil \frac{l_{ri}}{\overline{e}_{ri}} \right\rceil + d_{ri}) \tag{40}$$

$$\overline{\tau}_y = \sum_{r\in R}\sum_{i\in I_r} k_{yri}(\left\lfloor \frac{l_{ri}}{\underline{e}_{ri}} \right\rfloor + d_{ri}) + 6 \sum_{<r,i,s,j>\in Q} k_{yrisj}. \tag{41}$$

Newly defined big-M's:

M_{pqy}	Big-M for linearization.

Newly defined variables:

$\varphi_{ypq}, \overline{\varphi}_{ypq}$	non-negative variables to represent the value of $(\tau_y - T_{pq})^+$. More specifically, if $\tau_y - T_{pq} \ge 0$, we have $\varphi_{ypq} = \tau_y - T_{pq}$ and $\overline{\varphi}_{ypq} = 0$; if $\tau_y - T_{pq} < 0$, we have $\varphi_{ypq} = 0$ and $\overline{\varphi}_{ypq} = T_{pq} - \tau_y$.
Φ_{ypqt}	set to one if and only if $\varphi_{ypq} = t$, and zero otherwise.
Ψ_{ypqt}	set to the product of π_y with $(\tau_y - T_{pq})^+$ if and only if $(\tau_y - T_{pq})^+ = t$, and zero otherwise.

Newly defined constraints:

$$\tau_y - T_{pq} = \varphi_{ypq} - \overline{\varphi}_{ypq} \quad \forall p \in P, q \in P, y \in Y_{pq} \tag{42}$$

$$\varphi_{ypq} = \sum_{t \in T^{DEL}_{pqy}} t\phi_{ypqt} \quad \forall p \in P, q \in P, y \in Y_{pq} \tag{43}$$

$$\sum_{t \in T^{DEL}_{pqy}} \phi_{ypqt} = 1 \quad \forall p \in P, q \in P, y \in Y_{pq} \tag{44}$$

$$\psi_{ypqt} \ \geq \ t\pi_y + (\phi_{ypqt} - 1) \cdot M_{pqy} \quad \forall p \in P, q \in P, y \in Y_{pq}, t \in T^{DEL}_{pqy} \tag{45}$$

$$\varphi_{ypq}, \overline{\varphi}_{ypq} \ \geq \ 0 \quad \forall p \in P, q \in P, y \in Y_{pq} \tag{46}$$

$$\psi_{ypqt} \ \geq \ 0 \quad \forall p \in P, q \in P, y \in Y_{pq}, t \in T^{DEL}_{pqy} \tag{47}$$

$$\Phi_{ypqt} \in \{0, 1\} \quad \forall p \in P, q \in P, y \in Y_{pq}, t \in T^{DEL}_{pqy}. \tag{48}$$

The big-M in Constraints (45) can be set as $M_{pqy} = (\overline{\tau}_y - T_{pq})^+ \cdot n_{pq}$ as $t \leq (\overline{\tau}_y - T_{pq})^+$ and $\pi_y \leq n_{pq}$. Then the nonlinear penalty cost $\sum_{p \in P} \sum_{q \in P} \sum_{y \in Y_{pq}} \pi_y c^D_{pq} (\tau_y - T_{pq})^+$ in objective (4) is replaced with the linearized form $\sum_{p \in P} \sum_{q \in P} \sum_{y \in Y_{pq}} c^D_{pq} \sum_{t \in T^{DEL}_{pqy}} \Psi_{ypqt}$.

1.3. Linearization process of Constraints (20)

Constraints (20) contain a nonlinear part $\lambda_{rib}\eta_{r,i,(w-k) \bmod 7}$, which is the product of two binary variables. We define a new binary variable φ_{ribw} to replace the nonlinear part.

Newly defined variables:

φ_{ribw}	set to one if and only if the ship arrives at the berth b on the day w of a week in the i^{th} port of call on ship route r, and zero otherwise.

Then Constraints (20) become:

$$\sum_{r \in R'_p} \sum_{v=1}^{\overline{D}} \sum_{i \in I'_{rp}: d_{ri} = v} \sum_{k=0}^{v-1} \varphi_{r,i,b,(w-k+7) \bmod 7} \ \leq \ g_{bw} \quad \forall p \in P, b \in B_p, w \in W. \tag{49}$$

In addition, some more constraints need to be defined so that the newly defined variable φ_{ribw} can replace the function of $\lambda_{rib}\eta_{riw}$:

$$\varphi_{ribw} \geq \lambda_{rib} + \eta_{riw} - 1 \quad \forall r \in R, i \in I_r, b \in B_p, w \in W \tag{50}$$

$$\varphi_{ribw} \leq \lambda_{rib} \quad \forall r \in R, i \in I_r, b \in B_p, w \in W \tag{51}$$

$$\varphi_{ribw} \leq \eta_{riw} \quad \forall r \in R, i \in I_r, b \in B_p, w \in W \tag{52}$$

$$\varphi_{ribw} \in \{0,1\} \quad \forall r \in R, i \in I_r, b \in B_p, w \in W. \tag{53}$$

After applying the above linearization methods, model [M1] becomes [M2]:

$$\begin{aligned}
[\boldsymbol{M2}] \quad \text{Minimize Z} = & \underbrace{\sum_{r\in R}[m_r^S(\beta_r^{SP}+\beta_r^S)+m_r^P(\beta_r^{SP}+\beta_r^P)+c_r^{SP}\beta_r^{SP}+c_r^S\beta_r^S+c_r^P\beta_r^P+c_r^{\phi}\beta_r^{\phi}]}_{\textit{initial investment and operating cost of ships}} \\
& + \underbrace{\sum_{r\in R}\sum_{i\in I_r}[\frac{\beta_r^P+\beta_r^{\phi}}{h_r}f_{ri}^1(\gamma_{ri})+\frac{\beta_r^{SP}+\beta_r^S}{h_r}f_{ri}^2(\gamma_{ri})]}_{\textit{fuel cost}} + \underbrace{\sum_{p\in P}\sum_{q\in P}\sum_{y\in Y_{pq}}c_y^T\pi_y}_{\textit{transshipment cost}} \\
& + \underbrace{\sum_{p\in P}\sum_{q\in P}\sum_{y\in Y_{pq}}c_{pq}^D\sum_{t\in T_{pqy}^{DEL}}\Psi_{ypqt}}_{\textit{service level related penalty}} + \underbrace{\sum_{r\in R}\sum_{i\in I_r}\sum_{n=0}^{h_r}\frac{c_p^B\alpha_{rin\hat{b}}n}{h_r}}_{\textit{extra cost for berths without shore power}}
\end{aligned} \tag{54}$$

subject to (5)–(19), (21)–(39), (42)–(53). □

Appendix 3: Model reformulation 2

The model [M2] still has one nonlinear part "fuel cost function". We further linearize this nonlinear part. The specific transformation process of model [M2] is summarized below.

The fuel cost "$\sum_{r\in R}\sum_{i\in I_r}[\frac{\beta_r^P+\beta_r^\phi}{h_r}f_{ri}^1(\gamma_{ri})+\frac{\beta_r^{SP}+\beta_r^S}{h_r}f_{ri}^2(\gamma_{ri})]$" in the objective function contains the product of variable $(\beta_r^P+\beta_r^\phi)$ with the variable $f_{ri}^1(\gamma_{ri})$, and the product of variable $(\beta_r^{SP}+\beta_r^S)$ with the variable $f_{ri}^2(\gamma_{ri})$. To linearize this form, some newly defined variables and constraints are added as follows.

Newly defined indices and sets:

d	index of the number of days, which represents a leg's sailing time.
D_{ri}	set of possible numbers of days for the sailing time of leg $<r,i>$.
n	index of the number of ships with only shore power and ships without scrubbers or shore power, $n\in\{0,1,\cdots,\lvert h_r\rvert\}$.

Newly defined variables:

χ'_{rid}	set to one if and only if the sailing time in the i^{th} leg on route r is d, and zero otherwise.
χ^1_{rind}	set to one if and only if the number of ships with only shore power and ships without scrubbers or shore power in the i^{th} leg on route r is n^1 and the sailing time of leg $<r,i>$ is d, and zero otherwise.
χ^2_{rind}	set to one if and only if the number of ships with only scrubbers and ships with scrubbers and shore power in the i^{th} leg on route r is n^2 and the sailing time of leg $<r,i>$ is d, and zero otherwise.

In addition, some new constraints are defined.

Newly defined constraints:

$$d\sum_{d\in D_{ri}}\chi'_{rid}=\gamma_{ri}\quad\forall r\in R,i\in I_r \tag{55}$$

$$\sum_{d\in D_{ri}}\chi'_{rid}=1\quad\forall r\in R,i\in I_r \tag{56}$$

$$\chi'_{rid} \in \{0,1\} \qquad \forall r \in R, i \in I_r, d \in D_{ri} \tag{57}$$

$$\sum_{n=0}^{h_r} \sum_{d \in D_{ri}} \chi^1_{rind} = 1 \qquad \forall r \in R, i \in I_r \tag{58}$$

$$\sum_{n=0}^{h_r} \chi^1_{rind} = \chi'_{rid} \qquad \forall r \in R, i \in I_r, d \in D_{ri} \tag{59}$$

$$\sum_{n=0}^{h_r} \sum_{d \in D_{ri}} \chi^1_{rind} n^1 \leq \beta^P_r + \beta^\phi_r \qquad \forall r \in R, i \in I_r \tag{60}$$

$$\sum_{n=0}^{h_r} \chi^1_{rind} n^1 \geq \beta^P_r + \beta^\phi_r + (\chi_{rid} - 1)M \qquad \forall r \in R, i \in I_r, d \in D_{ri} \tag{61}$$

$$\chi^1_{rind} \in \{0,1\} \qquad \forall r \in R, i \in I_r, n \in \{0, \cdots, h_r\}, d \in D_{ri} \tag{62}$$

$$\sum_{n=0}^{h_r} \sum_{d \in D_{ri}} \chi^2_{rind} = 1 \qquad \forall r \in R, i \in I_r \tag{63}$$

$$\sum_{n=0}^{h_r} \chi^2_{rind} = \chi'_{rid} \qquad \forall r \in R, i \in I_r, d \in D_{ri} \tag{64}$$

$$\sum_{n=0}^{h_r} \sum_{d \in D_{ri}} \chi^2_{rind} n^2 \leq \beta^{SP}_r + \beta^S_r \qquad \forall r \in R, i \in I_r \tag{65}$$

$$\sum_{n=0}^{h_r} \chi^2_{rind} n^2 \geq \beta^{SP}_r + \beta^S_r + (\chi_{rid} - 1)M \qquad \forall r \in R, i \in I_r, d \in D_{ri} \tag{66}$$

$$\chi^2_{rind} \in \{0,1\} \qquad \forall r \in R, i \in I_r, n \in \{0, \cdots, h_r\}, d \in D_{ri}. \tag{67}$$

If leg i of route r covers ECAs, we have:

$$f^1_{ri}(d) = \begin{cases} a(d - T^0_{ri})^{-b} \alpha_E (L^E_{ri})^{b+1} + a(T^0_{ri})^{-b} \alpha_N (L^N_{ri})^{b+1} & T'_{ri} \leq d < \hat{T}_{ri} \\ ad^{-b}(\alpha_E^{\frac{1}{b+1}} L^E_{ri} + \alpha_N^{\frac{1}{b+1}} L^N_{ri})^{b+1} & d > \hat{T}_{ri} \end{cases} \tag{68}$$

$$\forall r \in R, i \in I_r, d \in D_{ri}$$

$$f_{ri}^2(d) = ad^{-b}\alpha_N(L_{ri}^E + L_{ri}^N)^{b+1} \quad \forall r \in R, i \in I_r, d \in D_{ri}. \tag{69}$$

and if leg i of route r does not cover ECAs, we have:

$$f_{ri}^1(d) = f_{ri}^2(d) = ad^{-b}\alpha_N(L_{ri}^E + L_{ri}^N)^{b+1} \quad \forall r \in R, i \in I_r, d \in D_{ri}. \tag{70}$$

After applying the above linearization methods, model [M2] becomes [M3]:

$$\begin{aligned}
[\boldsymbol{M3}] \quad \text{Minimize Z} = & \underbrace{\sum_{r\in R}[m_r^S(\beta_r^{SP}+\beta_r^S) + m_r^P(\beta_r^{SP}+\beta_r^P) + c_r^{SP}\beta_r^{SP} + c_r^S\beta_r^S + c_r^P\beta_r^P + c_r^\phi\beta_r^\phi]}_{initial\ investment\ and\ operating\ cost\ of\ ships} \\
& + \underbrace{\sum_{r\in R}\sum_{i\in I_r}\sum_{n=0}^{h_r}\sum_{d\in D_{ri}}\frac{n}{h_r}(f_{ri}^1(d)\chi_{rind}^1 + f_{ri}^2(d)\chi_{rind}^2)}_{fuel\ cost} + \underbrace{\sum_{p\in P}\sum_{q\in P}\sum_{y\in Y_{pq}} c_y^T\pi_y}_{transshipment\ cost} \\
& + \underbrace{\sum_{p\in P}\sum_{q\in P}\sum_{y\in Y_{pq}} c_{pq}^D \sum_{t\in T_{pqy}^{DEL}} \Psi_{ypqt}}_{service\ level\ related\ penalty} + \underbrace{\sum_{r\in R}\sum_{i\in I_r}\sum_{n=0}^{h_r}\frac{c_p^B\alpha_{rin\hat{b}}n}{h_r}}_{extra\ cost\ for\ berths\ without\ shore\ power}
\end{aligned} \tag{71}$$

subject to (5)–(19), (21)–(39), (42)–(53), (55)–(67).

Appendix 4: Brief introduction to the PSO algorithm used in comparative experiments

The model [M2] after the fuel cost function transformation may be tractable by CPLEX directly for some small-scale instances. However, large-scale instances cannot be solved by CPLEX within a reasonable time, or can lead to an out of memory error. Inspired by the behavior of bird flying, PSO algorithm was first proposed by Eberhart and Kennedy (1995). The PSO algorithm is a population-based method that uses fitness values to evaluate the population and is able to update the population to achieve an optimal solution (Soleimani and Kannan, 2015). Each particle has a position and velocity representing a solution. The position reflects the quality of the solution, and the velocity determines where the particle will move in the next iteration. Considering the ith particle in a n-dimensional space, its position and velocity at iteration k are denoted by $X_i(k) = (x_i^1(k), x_i^2(k), \cdots, x_i^n(k))$ and $V_i(k) = (v_i^1(k), v_i^2(k), \cdots, v_i^n(k))$, respectively. The updating velocity and position on the d-dimension of the particle i at the iteration $k+1$ are as follows:

$$v_i^d(k+1) = w \cdot v_i^d(k) + c_1 \cdot r_1 \cdot \left(Pbest_i^d(k) - x_i^d(k)\right) + c_2 \cdot r_2 \cdot \left(Gbest^d(k) - x_i^d(k)\right) \tag{72}$$

$$x_i^d(k+1) = x_i^d(k) + v_i^d(k+1). \tag{73}$$

where w is the inertial weight to control the impact of the previous history of velocity. c_1 and c_2 are the cognition learning factor and the social learning factor, respectively. r_1 and r_2 are random numbers in the interval $[0,1]$, which are in line with the setting used in related works (Deng et al., 2017; Chen et al., 2019). $Pbest_i^d(k)$, called the particle best solution, represents the best solution found by the ith particle itself till iteration k. $Gbest^d(k)$, called the global best solution, represents the global best solution found by all particles till iteration k. We set the parameter values of PSO algorithm as follows: $w = \frac{1}{2\ln 2}, c_1 = c_2 = 2$, which are consistent with related works (Shi and Eberhart, 1998; Nasir et al., 2012; Chen et al., 2019). The maximum iteration and population size are set to 35 and 55, respectively.

PSO algorithm starts by generating initial particles (solutions) with random speeds and locations, which represent the numbers of different types of ships on all routes. At each iteration, each particle tries to optimize its position and speed. Hence, they can optimize themselves using Eqs. (72) and (73) (Shi, 2001; Clerc, 2010). The algorithm continues as long as the best located position by each particle coincides with the best found location by other particle swarm. In other words, all particle swarms are concentrated in one point in space once the optimized solution to the problem has been achieved.